

Design and  
Verification Testing  
RPSEA 07121-1401  
Composite-reinforced  
Steel Drilling Riser

Final Report  
Revision A

30 September, 2011

Lincoln Composites, Inc.  
A Member of Hexagon Composite Group

Chad A. Cederberg



## Legal Notice

This report was prepared by Lincoln Composites, Inc., a member of Hexagon Composites Group, as an account of work sponsored by the Research Partnership to Secure Energy for America, RPSEA. Neither RPSEA, members of RPSEA, the National Energy Technology Laboratory, the U.S. Department of Energy, nor any person acting on behalf of any of the entities:

- a. Makes any warranty or representation, express or implied with respect to accuracy, completeness, or usefulness of the information contained in this document, or that the use of any information, apparatus, method, or process disclosed in this document may not infringe privately owned rights, or
- b. Assumes any liability with respect to the use of, or for any and all damages resulting from the use of, any information, apparatus, method, or process disclosed in this document.

This is a final report. Any data, calculations, information, conclusions, and/or recommendations reported herein are the property of the U.S. Department of Energy.

Reference to trade names or specific commercial products, commodities, or services in this report does not represent or constitute an endorsement, recommendation, or favoring by RPSEA or its contractors of the specific commercial product, commodity, or service.

## Executive Summary

As industry moves into deeper water, supporting the weight of a steel riser becomes a major design issue. The problem is further exacerbated when high pressure reservoirs are encountered and thick-wall risers are needed. Drilling, completion, and production of ultra-deepwater high pressure wells can benefit from risers constructed with lightweight composite materials.

One solution that appears to have significant potential is steel pipe over-wrapped with carbon fiber epoxy. This technology is not new and has been used in various military and commercial applications, and recently in choke and kill lines of low pressure Mobile Offshore Drilling Unit (MODU) drilling risers. Investigations into this type of construction for a high pressure drilling riser suggest a potential system weight savings of 40-50 % in comparison to conventional steel risers. This technology also shows promise in that it can be used with lower strength X80 steel, where weld-on couplers are either desirable or necessary.

In the case of a single high pressure drilling riser for tension-leg (TLP) or spar based operations, this is considered enabling technology. Such a design also allows the continued use of pipe materials and wall thicknesses within established and accepted manufacturing capabilities, without the need for new untested high-strength steels and large bore threaded connectors.

The business case for pursuing this technology is in the ability to perform dry tree TLP or spar based drilling and sidetrack operations, which may lead to substantial savings over comparable deepwater MODU operations with a differential approaching 500 M USD per day, or up to 50 MM USD on a single 100-day well. Additionally, safe and reliable lightweight risers for both wet and dry tree solutions reduce platform and life cycle costs.

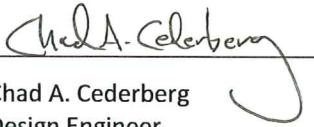
The work product of RPSEA project 07121-1401 is a composite-reinforced steel dry tree drilling riser design, having ultra-deepwater and high pressure well capability, and suitable for existing TLP or spar platforms using industry standard equipment. Under this project, a composite riser joint was designed and analyzed. The expected weight savings was confirmed. Three full-diameter prototypes were fabricated to demonstrate manufacturability, and tested to demonstrate sufficient margins of safety with respect to burst strength, bending fatigue, and tolerance to dropped object impact damage.

## Change History


30 September, 2011 A

Initial Release

Prepared by:

  
Chad A. Cederberg  
Design Engineer

Approved by:

  
Donald B. Baldwin  
Director, Product Development



## TABLE OF CONTENTS

1. Introduction .....	1
2. Background .....	2
Composites.....	2
Filament Winding .....	2
Lincoln Composites .....	3
3. Functional Specification .....	4
4. Applicable Standards.....	5
5. Project Workflow .....	6
6. Design Concept .....	7
7. Joint Construction .....	8
Steel Assembly .....	8
Composite Over-wrap .....	10
Autofrettage .....	14
Weight and Estimated Cost .....	15
8. Design and Analysis .....	16
Riser Configuration.....	16
Global Analysis .....	19
Local Analysis .....	23
Cyclic Fatigue.....	39
9. Design Verification .....	41
Prototype Configuration .....	41
Test Program .....	43
10. Conclusion .....	47

## LIST OF TABLES

Table 3-1: Design Requirements .....	4
Table 7-1: Properties of X80M PSL2 Steel Pipe .....	8
Table 7-2: Chemical Composition of X80M PSL2 Steel Pipe .....	8
Table 7-3: Tolerances of X80M PSL2 Steel Pipe .....	8
Table 7-4: Properties of F22 End Coupler .....	9
Table 7-5: Chemical Composition of F22 End Coupler .....	9
Table 7-6: Steel Assembly Summary .....	10
Table 7-7: Properties of Carbon Fiber Roving .....	11
Table 7-8: Properties of Neat Epoxy .....	11
Table 7-9: Composite Laminate Schedule .....	12
Table 7-10: Riser Joint Summary .....	14
Table 8-1: Riser Stack-up Listing .....	18
Table 8-2: Riser Tension Profiles .....	19
Table 8-3: Riser Internal Pressure Profiles .....	20
Table 8-4: Design Load Case Matrix .....	21
Table 8-5: Load Category, Frequency, and Duration .....	21
Table 8-6: Composite Fiber Stress Summary .....	35
Table 8-7: Allowable Steel Pipe Stress .....	36
Table 8-8: Steel Pipe Stress Summary .....	36
Table 8-9: Hoop and Axial Components of Pipe Stress .....	37
Table 8-10: Allowable Steel End Coupler Stress .....	38
Table 8-11: Steel End Coupler Stress Summary .....	38
Table 8-12: Pipe Fatigue Summary .....	40
Table 9-1: Prototype Measurements .....	42

## LIST OF FIGURES

Figure 5-1: Project Workflow Diagram .....	6
Figure 6-1: Multiple Traplock MCI (U.S. Patent 6,042,152).....	7
Figure 7-1: Joint Weight Breakdown .....	15
Figure 7-2: Estimated Joint Cost .....	15
Figure 8-1: Riser Stack-up Diagram .....	16
Figure 8-2: Load Sequencing .....	22
Figure 8-3: Local Analysis FE Model .....	24
Figure 8-4: Autofrettage – Tube Body.....	26
Figure 8-5: Factory Acceptance Test – Tube Body .....	26
Figure 8-6: Post Cure Interface Pressure .....	27
Figure 8-7: Autofrettage – Steel Stress.....	27
Figure 8-8: Post Autofrettage Interface Pressure.....	28
Figure 8-9: Post Autofrettage – Steel Stress.....	28
Figure 8-10: Autofrettage – Hoop Fiber Stress.....	29
Figure 8-11: Autofrettage - Axial Fiber Stress .....	29
Figure 8-12: Field Pressure Test – Tube Body .....	31
Figure 8-13: Normal Operating – Tube Body.....	31
Figure 8-14: Hydrostatic Collapse – Tube Body.....	32
Figure 8-15: Gas Kick – Tube Body .....	32
Figure 8-16: Mooring Failure – Tube Body .....	33
Figure 8-17: +M Top Mooring Failure – Steel Stress .....	33
Figure 8-18: –M Top Hydrostatic Collapse - Hoop Fiber Stress .....	34
Figure 8-19: –M Top Hydrostatic Collapse - Axial Fiber Stress .....	34
Figure 8-20: Strain-life Fatigue Curve .....	39
Figure 9-1: Prototype End Coupler.....	41
Figure 9-2: Full-diameter Prototype.....	42
Figure 9-3: Pressure Cycling – Tube Body .....	43
Figure 9-4: Pressure Cycling – Surface Strain v. Pressure.....	44
Figure 9-5: Combined Tension-Bending Cycle Test .....	45
Figure 9-6: Burst Carcass .....	45
Figure 9-7: Dropped Object Impact Test .....	46

## 1. Introduction

Lincoln Composites Inc., a member of Hexagon Composites Group (OSL:HEX), has been contracted by the Research Partnership to Secure Energy for America (RPSEA) to design a top-tensioned (TTR) dry tree drilling riser system using composite materials as a principal structural member, for the purpose of reinforcing conventional steel riser technology for ultra-deepwater and high pressure applications.

Scaling-up conventional steel risers has a prohibitive impact on riser weight by imposing significant demands on the surface facility. Increases in riser weight require a corresponding increase in tensioning capability, size of equipment, and structural capacity of the supporting platform; making necessary larger and more expensive floating structures. In addition to the costs associated with supporting a heavier riser, existing fabrication methods may not be feasible at the required wall thickness.

An alternative to accommodating heavier steel risers is to reinforce existing riser constructions with high-strength and lightweight composite materials. By virtue of a much higher specific strength, an equivalent increase in X80 pipe thickness can be made with composite materials at one-fifth of the weight. In addition, design methods from the pressure vessel industry for optimizing utilization and reliability of composite over-wrapped metal pressure vessels (COPV) may also be applied to composite risers to further improve performance. Preceding investigations suggest a potential system weight savings of 40-50 % for such a design. It is for this reason composite risers are being looked at as a cost-effective solution to access ultra-deepwater wells currently impractical to develop.

The objective of this project is to develop and commercialize a lightweight dry tree drilling riser system for ultra-deepwater and high pressure that is suitable for existing tension-leg (TLP) or spar platforms using industry standard equipment. The project has been planned in phases; beginning with design and verification testing (phase 1), followed by design qualification, field demonstration, and ending with commercialization.

Funding for phase 1 is provided through the NETL/RPSEA ultra-deepwater program under project 07121-1401 *Composite Riser for Ultra-deepwater High Pressure Wells*. Lincoln Composites is the primary performer with analytical support and testing services provided by Stress Engineering Services. The project started in January 2009 and was completed in September 2011. Contract value including industry matching was 2.7 MM USD.



## 2. Background

### Composites

A composite material is one consisting of two or more distinct phases of different physical or chemical properties, which at a macroscopic scale, offer unique properties neither of the constituents possess. In this report, the term composite is used to refer to a class of advanced materials constructed of high-strength fibrous reinforcements in a polymeric matrix (i.e. polymer matrix composites, PMC). Specifically, PAN-based carbon fiber reinforced epoxy.

Carbon fiber is a man-made material produced by controlled pyrolysis of a polyacrylonitrile (PAN) precursor, a synthetic fiber commonly used in textiles. A single carbon fiber filament is seven microns in diameter, is effectively infinite in length, and exhibits a tensile strength many times that of high-strength steel. Thousands of filaments are bundled together to form roving, and spooled into bobbins. A variety of different grades of fiber are available from manufacturers such as Hexcel, Toray, Toho, and Grafil; with properties tailored to meet a variety of different strength and/or stiffness requirements.

An epoxy is a thermosetting polymer formed by the reaction of an epoxide resin with a polyamine curing agent. This two-part system is mixed as liquids, sometimes with additives to enhance certain properties. Many of the epoxies used in high-performance composites require curing with heat to fully crosslink and develop the desired mechanical properties and environmental/chemical stability.

Like yarns in textiles, carbon fiber roving is very strong and stiff along its length but otherwise has no real shape. To be useful as a structural material, the roving requires a substantive binder (or matrix) to support the fibers in compressive and shear loadings. This is the function of the epoxy. While liquid, it penetrates and fills the interstitial spaces between fiber filaments. When cured, it results in a very tough second phase that gives the composite a solid form.

### Filament Winding

Filament winding is a composite fabrication method for constructing generally cylindrical structures. The process involves winding a continuous band of roving, pulled from bobbins under controlled tension and wetted with epoxy, over the surface of a part or temporary mandrel. Typically, the part being over-wrapped rotates about its principal axis as a winding head traverses back and forth along it, laying down a band of composite material in a prescribed pattern. This pattern is repeated with rotational indexing so that with each circuit of the winding head the band of roving lays adjacent to preceding bands, until the surface is fully covered, making a layer of composite material. When winding is complete, the epoxy is cured by heating the part in an oven.

Due to the bi-directional nature of the winding band, having fiber dominant properties in the direction of the fiber and matrix dominant properties across, in-plane properties of composite layers are also orthotropic. The level of layer orthotropy (relative strength along meridional and circumferential lines) is governed by its fiber angle. The orthotropy (or bias) of each layer, the number of layers, and sequencing of layers is an essential part of laminate design. By tailoring the laminate, a structure can be designed orienting strengths according to applied loads. For this reason a filament-wound composite structure is uniquely suited to top-tensioned and high pressure risers.

---

This introduction to composites and filament winding are to provide context for material presented later in this report. It is a narrow and simplistic view of a broad and complex subject. For more information, ASM Handbook Volume 21 *Composites* (ISBN 9780871707031) is recommended.

## **Lincoln Composites**

Established in 1963 as a manufacturing plant for the Polaris ICBM motor case, Lincoln Composites has grown to become a world leader in the design and manufacture of filament-wound composite structures. Founded within the Defense Division of Brunswick Corporation, its core technology developed alongside leading government research and advancements in composites for the aerospace and defense industries. Lincoln Composites applied this knowledge with particular focus on filament-wound structures to develop a portfolio of lightweight products for the military; including rocket motor cases for tactical and strategic missiles, launch tubes, pressure vessels, aircraft fuel tanks, and satellite structures.

Lincoln Composites started to explore new applications for its technology in response to declining government funding in defense related programs after the collapse of the Soviet Union. Around the turn of the century a new business unit was established to develop and market lightweight products for the automotive and oil and gas industries. Among its product developments are pressure vessels for natural gas and hydrogen fuel cell vehicles, accumulators for hydraulic regenerative braking systems, MEGS bulk gas transport modules, flexible drill pipe and drillable casing, and accumulators for offshore riser tensioning. In 2005, the commercial products group was purchased by Hexagon Composites, a Norwegian owned company with a similar commercial focus.

## **Riser Development Projects**

Over the past fifteen years Lincoln Composites has played an instrumental role in industry efforts to develop composite risers.

In 1995, the U.S. Department of Commerce National Institute of Standards and Technology (NIST) Advanced Technology Program (ATP) assembled a joint industry project with the goal to design, fabricate, test, and qualify a composite production riser. Lincoln Composites was selected for design and prototype fabrication. The design was based on 10 ¾ inch casing size and constructed of a carbon and glass fiber hybrid epoxy composite with an elastomeric liner and steel end connectors. The design was the first riser application to demonstrate the traplock metal-to-composite interface (MCI). Ninety prototypes were made. A comprehensive test program evaluated the design in tension, burst, collapse, and fatigue. From results, performance envelope and static/cyclic fatigue curves were developed. The project demonstrated a successful design.

Following the NIST-ATP project, Norske Conoco AS (NCAS) and Kvaerner Oilfield Products (KOP) contracted Lincoln Composites to design a similarly constructed 559 mm (22 inch) diameter drilling riser joint featuring a thin full-length titanium liner for the CompRiser project. The joint was designed to fit into the existing Heidrun TLP riser string with the intent of field demonstration. To be interchangeable with the existing titanium joints, the composite joint maintained similar stiffness properties and used the same end coupler design. After a successful qualification program, in July 2001 a joint was placed in service and used in drilling three live wells; being placed at different positions in the riser string for each well. The composite joint was successful in its demonstration and was later taken over by the Heidrun operator and used to drill additional wells.

Lincoln Composites' most recent work has been a 368 mm (14.5 inch) diameter ultra-deepwater and high pressure drilling riser for Shell Global Solutions. It was a load-sharing design based on a steel riser over-wrapped with carbon fiber epoxy composite. Two prototypes were made for evaluation. The first burst tested. The second was subjected to 100 000 bending cycles representative of a 100-year hurricane storm, followed by ten pressure cycles to rated pressure before being pressurized to burst. Both prototypes demonstrated a burst pressure in excess of 206,8 MPa (30,000 psi). The configuration proposed to RPSEA for this project was based on this design.



### 3. Functional Specification

At project kick-off, the project working committee met to establish an initial set of requirements for sizing the riser. The resulting list is presented in Table 3-1 followed by additional statements made concerning design.

**Table 3-1: Design Requirements**

	SI	USC
Water Depth	3 048 m	10,000 ft
Pressure Rating	103,4 MPa	15,000 psi
Top-tension Capability	13,3 MN	3,000 kipf
Outside Diameter (with buoyancy) <sup>1</sup>	1 524 mm	60 inch
Drift Diameter	495,3 mm	19.5 inch
Service Life	20 Years	
Temperature Rating	82 °C	180 °F

<sup>1</sup> Size to fit through a 60 inch rotary table opening

To make use of industry standard equipment, the riser and buoyancy are to be compatible with a tensioning system capable of 13,3 MN (3,000 kipf) and be sized to fit through a 60-inch rotary table opening. To give operators flexibility in drilling equipment, the riser shall have a minimum drift diameter of 495,3 mm (19.5 inch).

#### Bore Abrasion and Wear

Composites have long been recognized as having great potential for reducing weight of marine risers. However, for composite risers to be accepted for drilling applications, wear and abrasion of the bore must be addressed. The soft elastomer and thermoplastic liners, or relatively thin metal liners used in past designs may erode, tear, or be gouged by the drill string or by cuttings carried in drilling fluids. For this reason a design based on reinforcing a conventional steel drilling riser was chosen for this project, providing an equivalently durable and fluid tight bore.

#### Chemical and Environmental Resistance

Compatibility with chemicals common to offshore drilling operations and the effects of a marine environment on the riser design must be considered.

The following list of considerations was provided by NCAS/KOP for the CompRiser project and is repeated here for reference. Chemical compatibility shall consider exposure to fluids common to marine drilling operations, such as, seawater, oil and water based muds, sodium chloride or calcium chloride, hydrochloric acid, raw hydrocarbons, hydrogen sulfide, methanol and glycol, demulsifiers, corrosion and scale inhibitors, and biocides. Environmental factors include prolonged UV exposure, extreme temperature, and the effects of marine growth.

#### Impact Resistance

The riser shall remain in a working condition after sustaining a 68 kJ (50 kipf-ft) impact from a dropped object without protection. This energy is consistent with data related to the CompRiser project (Heidrun) for a steel casing joint falling off the platform and into the water, impacting the riser at a depth below 50 m (164 ft).

#### **4. Applicable Standards**

Risers constructed with composite materials are relatively new and have limited guidance in the form of industry standards. With increased interest in composite technology as a means of reducing riser weight, however, efforts to develop appropriate standards are beginning to take shape. Most notably DNV RP-F202 *Composite Risers*.

DNV RP-F202, OS-F201, and OS-C501, as well as API RP 2RD *Design of Risers for Floating Production Systems and Tension-Leg Platforms*, have been used as guiding documents for this project.

The project working committee included representation from the Bureau of Ocean Energy Management (BOEM), who provided design and testing guidance on details related to regulatory interests.



## 5. Project Workflow

A diagram illustrating major project steps and a summary of information is presented in Figure 5-1.

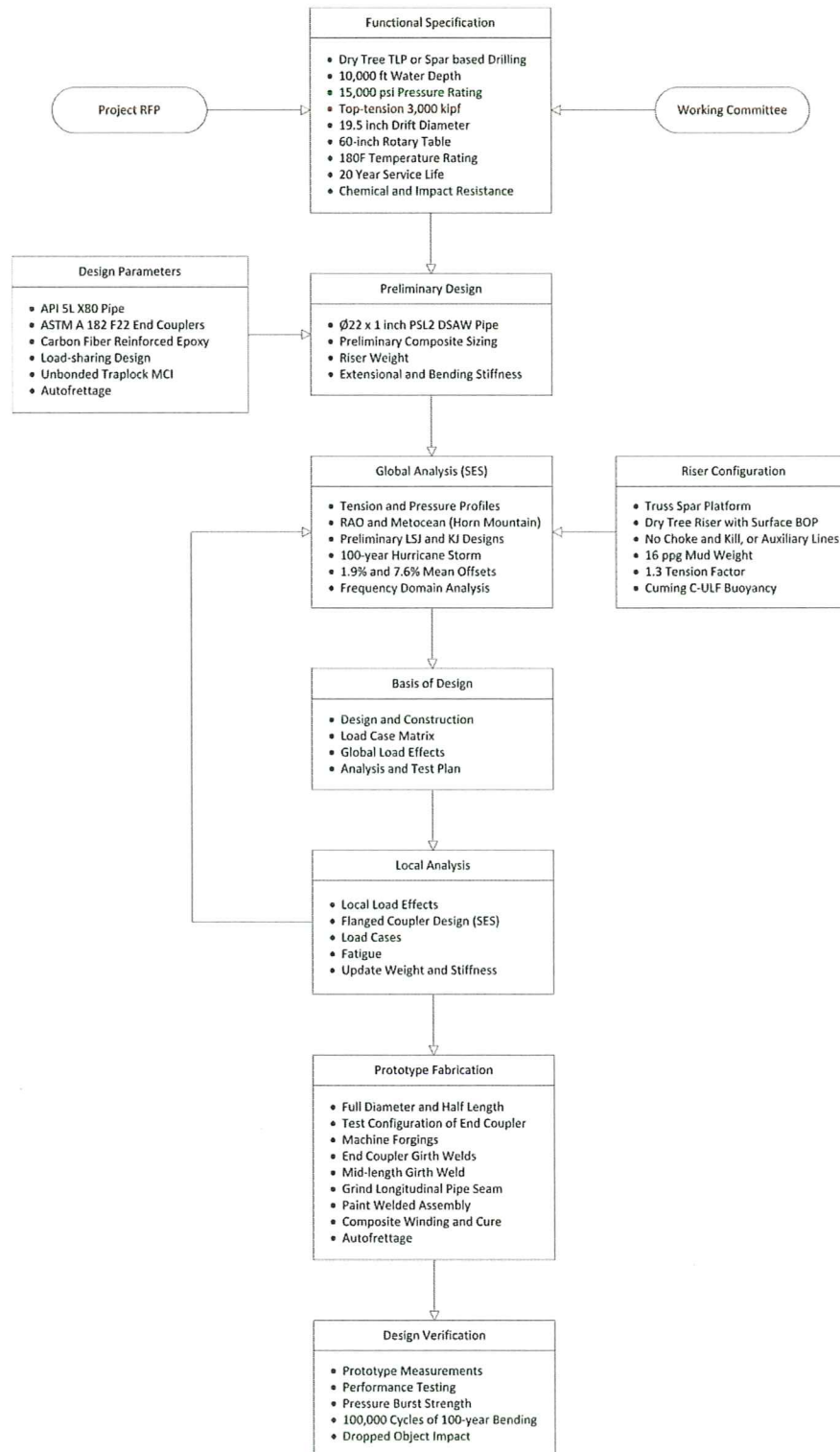


Figure 5-1: Project Workflow Diagram

## 6. Design Concept

The design proposed by Lincoln Composites is essentially a conventional steel riser over-wrapped with carbon fiber reinforced epoxy, combining a durable and fluid tight bore with the efficiency of high-performance composites.

Like a conventional riser, the steel component is an assembly of two end couplers welded to each end of straight pipe. Design of the riser is based on  $\varnothing 559 \times 25,4$  mm ( $\varnothing 22 \times 1$  inch) API 5L grade X80 line pipe. End couplers consists of a flange<sup>1</sup>, a cylindrical extension for handling the joint and for engaging with the spider, a series of circumferential grooves related to the MCI, and a radiused taper transitioning to an end dimension that can be welded to pipe. End couplers are welded to pipe using a single-side Submerged Arc Welding (SAW) process.

The steel assembly is over-wrapped with composite using an automated filament winding process. The composite structure is a multi-layered, angle-ply laminate formed by winding successive layers of continuous carbon fiber roving, under controlled tension and wetted with epoxy, over the steel and subsequent curing with heat. The thickness and laminate schedule of the composite are determined based on required hoop and axial strengths.

The sharing of riser tension, bending, and pressure end loads between the steel assembly and the composite is accomplished through the metal-to-composite interface (MCI). For this design, the MCI is a purely mechanical connection made by winding composite around circumferential grooves at both ends of the joint. After cure, the composite is solid, and forces applied to the joint flanges are shared with the composite as the mating groove geometry bear out (through contact pressure). The name commonly associated with this type of MCI is a traplock design. The particular configuration developed by Lincoln Composites is one that does not make use of adhesive bonding<sup>2</sup>. An illustration of the end coupler design and traplock MCI is presented in Figure 6-1.

To protect the composite from the environment<sup>3</sup> and to prevent a galvanic couple from developing between the carbon fiber and steel, the composite is jacketed in a 0,8 mm (30 mil) thick layer of hydrogenated nitrile butadiene rubber (HNBR). The inner layer of HNBR also provides a secondary barrier for containment of drilling fluids if a fatigue crack developed in the steel or its welds. To protect the outer layer of HNBR from damage a sacrificial glass fiber reinforced epoxy wear surface is wound overtop. Over this, a polyurethane paint topcoat is applied.

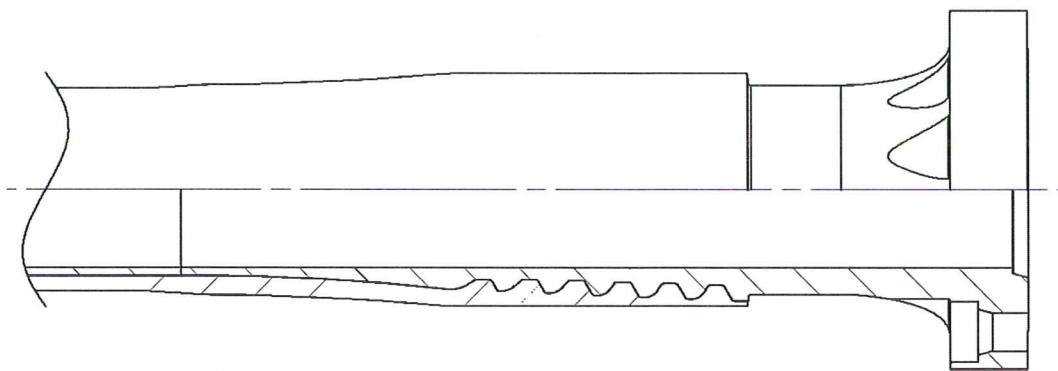


Figure 6-1: Multiple Traplock MCI (U.S. Patent 6,042,152)<sup>4</sup>

<sup>1</sup> A flanged end coupler was chosen by the RPSEA working committee for this project; however, the design can accept other connector types.

<sup>2</sup> The elevated temperature necessary to cure the epoxy will result in a post cure radial tension at the interface if bonded due the difference in CTE between steel and composite. This tension would likely tear apart the inner layer of HNBR.

<sup>3</sup> The composite is fully compatible with seawater and the HNBR jacket is not required to be water tight. The outer layer of HNBR provides an additional measure of chemical and mechanical protection by buffering the composite from surface damage.

<sup>4</sup> This design utilizes a patented multiple traplock MCI. Lincoln Composites is sole owner of this patent, for which there are no licenses.

## 7. Joint Construction

### Steel Assembly

The steel assembly of the riser joint consists of a  $\varnothing 559 \times 25,4$  mm ( $\varnothing 22 \times 1$  inch) API 5L grade X80M PSL2 pipe tube body with weld-on end couplers made of a modified ASTM A 182 grade F22 low alloy steel.

#### Pipe Tube Body

The pipe is formed by the UOE process, having a single longitudinal DSAW weld seam. The longest this pipe can be manufactured is in 13,7 m (45 ft) lengths. For a 22,9 m (75 ft) joint, the necessary length of pipe is 17,3 m (56.8 ft), requiring a mid-length girth weld to make the tube body. Pipe mechanical properties, its chemical composition, and tolerances used in design are listed in Table 7-1, Table 7-2, and Table 7-3 respectively. Introduced in the 44<sup>th</sup> edition of API 5L is an additional provision for PSL2 pipe for offshore service (annex J). Although more restrictive in dimensional tolerances, it was not assumed in design.

The type, size, and grade of pipe used in design are based on assets available to the project for making design verification prototypes. Other pipe constructions may also be suitable.

**Table 7-1: Properties of X80M PSL2 Steel Pipe**

	SI	USC
Pipe Specification	API 5L Grade X80M PSL2 DSAW	
Outside Diameter	558,8 mm	22.00 inch
Wall Thickness	25,4 mm	1.00 inch
Pipe Weight	334,1 kg/m	224.5 lb/ft
Yield Strength <sup>1 2</sup>	555 MPa	80.5 ksi
Tensile Strength <sup>1</sup>	625 MPa	90.6 ksi
Yield to Tensile Strength Ratio	0.93 Maximum	
Elongation <sup>1</sup>	16 %	16 %
Tensile Modulus <sup>3</sup>	186 GPa	27 Msi
Reduction of Area <sup>3</sup>	77 %	77 %

<sup>1</sup> Minimum

<sup>2</sup> 0.5 % total extension yield strength

<sup>3</sup> Typical, based on testing of pipe purchased for prototyping

**Table 7-2: Chemical Composition of X80M PSL2 Steel Pipe**

C	Si	Mn	P	S	V	Nb	Ti	Cu	Ni	Cr	Mo	CE IIW	CE Pcm
0.12	0.45	1.85	0.025	0.015		Sum $\leq 0.15$		0.50	1.00	0.50	0.50	0.43	0.25

<sup>1</sup> Percent maximum mass fraction based on heat and product analyses

<sup>2</sup> For product analysis carbon mass fraction equal to or less than 0.12 % CE Pcm (Ito-Bessyo) applies, otherwise CE IIW

**Table 7-3: Tolerances of X80M PSL2 Steel Pipe**

	SI	USC
Outside Diameter	+/- 3,18 mm	+/- .125 inch
Roundness <sup>1</sup>	11,2 mm	.44 inch
Straightness <sup>2</sup>	34,6 mm	1.36 inch
Wall Thickness	+/- 1,52 mm	+/- .060 inch
Yield Strength	555 - 705 MPa	80.5 - 102.3 ksi
Tensile Strength	625 - 825 MPa	90.6 - 119.7 ksi

<sup>1</sup> Maximum difference between largest and smallest outside diameter

<sup>2</sup> Maximum deviation (taut line) based on 0.2 % for a 22,9 m (75 ft) joint having 17,3 m (56.8 ft) of pipe length



### Weld-on End Coupler

The end coupler is spindle forged, heat treated, and machined to finished dimensions. A modified grade F22 steel (restricted carbon) was chosen based on its ability to be hardened and suitability to welding with grade X80 pipe. End coupler mechanical properties and its chemical composition are listed in Table 7-4 and Table 7-5.

**Table 7-4: Properties of F22 End Coupler**

	SI	USC
Material Specification	Modified ASTM A 182 grade F22 (2-1/4CR-1MO)	
Length <sup>1</sup>	2 773 mm	109.2 inch
Wall Thickness <sup>2</sup>	87,1 mm	3.43 inch
Flange Diameter	1 168 mm	46.0 inch
Weight <sup>1</sup>	3 724 kg	8,210 lb
Weight of Seal Ring, Bolts, Inserts and Washers	815,1 kg	1,797 lb
Yield Strength <sup>3,4</sup>	517 MPa	75.0 ksi
Tensile Strength <sup>3</sup>	655 MPa	95.0 ksi
Elongation <sup>3</sup>	18 %	18 %
Reduction of Area <sup>3</sup>	35 %	35 %
Hardness	237 HBW (22 HRC) Maximum	

<sup>1</sup> Length and weight are per end

<sup>2</sup> Required forging thickness 108,8 mm (4.3 inch)

<sup>3</sup> Minimum

<sup>4</sup> 0.2 % offset yield strength

**Table 7-5: Chemical Composition of F22 End Coupler**

C		Mn		P	Si	S	Cr		Mo
0.10 – 0.15		0.30 – 0.60		0.015	0.50	0.013	2.00 – 2.50		0.87 – 1.13
Cu	Ni	Ti	V	Nb	V + Nb	N	Ca	H	CE IIW
0.35	0.50	0.002	0.020	0.010	0.025	0.012	0.005	0.0002	0.865 – 0.925

<sup>1</sup> Percent maximum mass fraction based on heat and product analyses

### Welding

The two pipe sections making the tube body are oriented to offset their longitudinal weld seams. End coupler and mid-length pipe-to-pipe girth welds are made using a single-side Submerged Arc Welding (SAW) process. Procedures for making both welds are established and have a successful history in deepwater and sour service applications. All three girth welds are conditioned inside and out, flush with the base material. The longitudinal pipe weld seam is also conditioned on the outside diameter to minimize reinforcement height; otherwise the profile of the weld bead would create a stress concentration in the composite.

### Anti-corrosion Coating

Following welding, all external surfaces of the steel assembly are blast cleaned and coated with a protective anti-corrosion material. A specific coating is not required and industry standard best practices should be used. The only consideration is any coating must be resistant to solvents; as a solvent-base release agent is applied to the surface to prevent bonding between the steel assembly and the inner HNBR layer. The use of solvents is also very prevalent in composite manufacturing to remove epoxy from equipment and tooling.

The combination of a coating, the galvanic isolation provided by HNBR, and a cathodic protection (CP) system in service, form the basis for mitigating corrosion of the exterior surface. Corrosion of the inside bore would be managed like any conventional riser.

Nominal properties of the steel assembly are listed in Table 7-6. Weight does not include an allowance for an anti-corrosion coating; however it is not expected to have a significant impact on joint weight.

**Table 7-6: Steel Assembly Summary**

	SI	USC
Joint Length	22,9 m	75 ft
Pipe Diameter	558,8 mm	22.00 inch
Pipe Thickness	25,4 mm	1.00 inch
Drift Diameter	495,3 mm	19.5 inch
Flange Diameter	1 168 mm	46.0 inch
Steel Weight	13 232 kg	29,172 lb
Weight of Coupling Hardware	815,1 kg	1,797 lb
Averaged Weight	614,5 kg/m	412.9 lb/ft
Averaged Wet Weight	534,2 kg/m	359.0 lb/ft

## Composite Over-wrap

### Release Agent

At the temperature necessary to cure the epoxy, the steel expands in size according to its coefficient of thermal expansion (CTE). It is with the steel at this size the epoxy will set and the composite take its shape. After completing cure, the part is air cooled to ambient temperature, and the steel returns to its original size. The composite, however, due to a much lower CTE does not contract the same amount. The difference, if the two were bonded, would result in radial tension at the interface that would likely tear apart the inner HNBR layer.

To ensure a clean separation of the steel assembly on post cure cooldown, the over-wrapped surfaces are coated with a release agent. To promote a uniform peeling away over the length of the joint, a spiral wrap of Teflon tape is applied overtop the release agent using a lead rate providing fifty percent surface coverage (like the stripe of a barber pole).

### Hydrogenated Nitrile Butadiene Rubber (HNBR) Layers

Two layers of HNBR are used to form a jacket around the structural composite; an inner layer applied overtop the steel assembly before winding, and an outer layer applied before winding the sacrificial glass fiber top layer. Both layers are made by hand laying 0,76 mm (30 mil) sheets of uncured calendared material. Seams between sheets are overlapped. To close the outboard ends, the inner layer is made longer than the area over-wrapped, is folded back after winding the structural composite (capping the end), and overlapped by the outer layer. The seam is covered by the sacrificial glass fiber composite wound overtop the outer HNBR layer. The temperature for curing the epoxy also (co-)cures the HNBR, fusing seams and bonding to the composite.

### Structural Carbon Fiber Composite

With the inner layer of HNBR in place, the steel assembly is over-wrapped with composite using a numerically controlled filament winding machine. The winding band is made up of several ends (tows) of carbon fiber roving, fed to the winder from a creel of tensioned bobbins, and impregnated with epoxy using a wet bath system located behind the eye of the winding head. Epoxy is added at an amount that adequately wets out the fiber, and then consolidated by kneading the band with a series of static bars. The size of the winding band is roughly 25 mm (1.0 inch) in width and 0,38 mm (.015 inch) thick.

Carbon fiber's high strength and low specific weight, its superior static and cyclic fatigue characteristics, and its resistance to chemical and environmental corrosion, make it a very efficient and reliable reinforcement. The fiber used in design is Toray T700SC-24000-50C, a 24k filament count polyacrylonitrile-based (PAN) standard modulus carbon fiber (SMCF), having a tensile strength of 4 826 MPa (700 ksi) or better. A higher strength SMCF fiber was chosen over other types as it offers the best value<sup>5</sup> in terms of cost and performance. This particular fiber is a staple of Lincoln Composites as it has the most favorable ratio of cost per unit of delivered strength in its class.

The epoxy is a 2-part system of diglycidyl ether of bisphenol F (DGEBF) and a non-MDA aromatic amine curing agent. It is a system proprietary to Lincoln Composites, developed for applications requiring exceptional strength and toughness, while maintaining a high level of chemical and environmental resistance. Its viscosity is suitable to filament winding and its pot life supports longer wind times. When cured at 149 °C (300 °F), the epoxy has a typical glass transition temperature (Tg) of around 138 °C (280 °F).

Typical material properties for carbon fiber roving and neat epoxy are listed in Table 7-7 and Table 7-8.

**Table 7-7: Properties of Carbon Fiber Roving**

	SI	USC
Fiber Manufacturer	Toray T700SC-24000-50C (PAN)	
Tensile Strength	5 171 MPa	750 ksi
Tensile Modulus	233,7 GPa	33.9 Msi
Elongation	2.1 %	2.1 %
Yield	603 m/kg	897 ft/lb
Specific Weight	1,80 gm/cm <sup>3</sup>	.065 lb/in <sup>3</sup>
Roving Section Area	0,92 mm <sup>2</sup>	.00143 in <sup>2</sup>
Coefficient of Thermal Expansion (CTE)	-0,38 10 <sup>-6</sup> /°C	-.21 10 <sup>-6</sup> /°F

**Table 7-8: Properties of Neat Epoxy**

	SI	USC
Material Specification	Bis-F Aromatic Amine Epoxy (Proprietary)	
Tensile Strength	78,6 MPa	11.4 ksi
Tensile Modulus	2,79 GPa	.39 Msi
Elongation	7 %	7 %
Cure Temperature	149 °C	300 °F
Glass Transition Temperature, Tg	138 °C	280 °F
Specific Weight	1,20 gm/cm <sup>3</sup>	.043 lb/in <sup>3</sup>
Coefficient of Thermal Expansion (CTE)	64,8 10 <sup>-6</sup> /°C	36.0 10 <sup>-6</sup> /°F
Water Absorption, % wt	2 %	2 %

A wet winding process was chosen over prepreg<sup>6</sup> roving as a cost control measure. Prepreg is typically used in applications where weight is critical and precise control of resin content is required to maximize the amount of fiber in the structure. The downside to prepreg is the cost of materials increase appreciably (potentially 2-4 times). For this design, prepreg is not recommended since the effect of variation in weight due to resin content is small and any benefits will be insignificant compared to the impact on affordability.

<sup>5</sup> The cost of composite is governed by its strength (the amount of fiber and epoxy used), its direct cost, and the time to wind it. Commercially available "low-cost carbon fibers" have a lower direct cost but substandard performance negates much of their savings by requiring more material and a longer wind time, and yields a heavier design. Premium aerospace fibers are very efficient but considerably more expensive.

<sup>6</sup> Prepreg is fiber where epoxy has been added and re-spooled offline, often requiring cold storage to prevent the epoxy from advancing.



Winding is performed in pattern sets, one set for each opposing trap pair of the MCI. With this design having six traps, there are six repeating pattern sets. Each set consisting of four hoop oriented layers interspersed by three axial layers. Winding begins with the innermost trap pair and progresses outward. The laminate schedule for winding is listed in Table 7-9. Fiber angle is with respect to the part meridian.

**Table 7-9: Composite Laminate Schedule**

Layer	Trap	Description	Fiber Direction	Fiber Angle, deg	Thickness, mm	Thickness, inch
1	1	Carbon Fiber/Epoxy	Hoop	80.00	1,62	.0636
2		Carbon Fiber/Epoxy	Axial	10.00	0,71	.0279
3		Carbon Fiber/Epoxy	Hoop	80.00	1,60	.0631
4		Carbon Fiber/Epoxy	Axial	10.00	0,70	.0276
5		Carbon Fiber/Epoxy	Hoop	80.00	1,59	.0626
6		Carbon Fiber/Epoxy	Axial	10.00	0,70	.0274
7		Carbon Fiber/Epoxy	Hoop	80.00	1,58	.0621
8	2	Carbon Fiber/Epoxy	Hoop	80.00	1,57	.0617
9		Carbon Fiber/Epoxy	Axial	10.00	0,69	.0271
10		Carbon Fiber/Epoxy	Hoop	80.00	1,56	.0612
11		Carbon Fiber/Epoxy	Axial	10.00	0,68	.0269
12		Carbon Fiber/Epoxy	Hoop	80.00	1,54	.0608
13		Carbon Fiber/Epoxy	Axial	10.00	0,68	.0266
14		Carbon Fiber/Epoxy	Hoop	80.00	1,53	.0603
15	3	Carbon Fiber/Epoxy	Hoop	80.55	1,61	.0635
16		Carbon Fiber/Epoxy	Axial	10.00	0,71	.0280
17		Carbon Fiber/Epoxy	Hoop	80.55	1,60	.0630
18		Carbon Fiber/Epoxy	Axial	10.00	0,71	.0278
19		Carbon Fiber/Epoxy	Hoop	80.55	1,59	.0625
20		Carbon Fiber/Epoxy	Axial	10.00	0,70	.0276
21		Carbon Fiber/Epoxy	Hoop	80.55	1,58	.0620
22	4	Carbon Fiber/Epoxy	Hoop	80.55	1,57	.0617
23		Carbon Fiber/Epoxy	Axial	10.00	0,69	.0272
24		Carbon Fiber/Epoxy	Hoop	80.55	1,56	.0612
25		Carbon Fiber/Epoxy	Axial	10.00	0,69	.0270
26		Carbon Fiber/Epoxy	Hoop	80.55	1,54	.0608
27		Carbon Fiber/Epoxy	Axial	10.00	0,68	.0269
28		Carbon Fiber/Epoxy	Hoop	80.55	1,53	.0604
29	5	Carbon Fiber/Epoxy	Hoop	81.05	1,61	.0634
30		Carbon Fiber/Epoxy	Axial	10.00	0,71	.0281
31		Carbon Fiber/Epoxy	Hoop	81.05	1,60	.0629
32		Carbon Fiber/Epoxy	Axial	10.00	0,71	.0279
33		Carbon Fiber/Epoxy	Hoop	81.05	1,59	.0625
34		Carbon Fiber/Epoxy	Axial	10.00	0,70	.0277
35		Carbon Fiber/Epoxy	Hoop	81.05	1,58	.0620
36	6	Carbon Fiber/Epoxy	Hoop	81.05	1,57	.0617
37		Carbon Fiber/Epoxy	Axial	10.00	0,70	.0274
38		Carbon Fiber/Epoxy	Hoop	81.05	1,56	.0613
39		Carbon Fiber/Epoxy	Axial	10.00	0,69	.0272
40		Carbon Fiber/Epoxy	Hoop	81.05	1,55	.0609
41		Carbon Fiber/Epoxy	Axial	10.00	0,69	.0270
42		Carbon Fiber/Epoxy	Hoop	81.05	1,54	.0605

<sup>1</sup> Layer fiber angle and thickness are nominal and represent the tube body section

<sup>2</sup> Fiber content 57.5 % by volume (1.74 bulk factor)

Winding of hoop and axial layers are at fiber angles of 80 deg and 10 deg respectively. While 90 deg and 0 deg might seem more appropriate, these angles cannot be easily produced by filament winding. A 90 deg winding would be unstable or the band would split over curved surfaces of the MCI, and 0 deg winding would bridge over the tube body. Having the fibers at a small angle to applied loads does not appreciably affect design efficiency.

One advantage of layers having an off-axis fiber angle is improved ductility. Off-axis fiber angles are wound by helical winding, which results in a layer twice the band thickness and having a basket weave like construction. Windings are placed at two angles, one positive and one negative, symmetric about the meridian. A positive angle is placed when the winding head is traveling in one direction along the part length, and a negative angle when its direction reverses. The two bands are interwoven, cross-reinforcing each other at regular intervals. When all the fibers of a layer are aligned (as in 90 deg and 0 deg winding), weak matrix dominant planes exist within the layer.

The fiber angle and thickness of each layer varies depending on parameters associated with winding. The two more important being the number of roving ends (tows) in the winding band and the number of pattern circuits giving full coverage (i.e. total length of the band). The number of tows establishes the width of the winding band. The number of pattern circuits is determined by dividing the local part circumference by the arc length of winding band crossing it for a given angle (e.g. lower angle windings require more circuits than higher angles). Since this must be an integer value, rounding down or up creates a gap or overlap condition respectively between adjacent bands. To minimize a gap or overlap, fiber angle is adjusted. The values listed in Table 7-9 represent an average thickness around the circumference. Laminate thickness and composite weight are based on a fiber content of 57.5 % and 5 % matrix voids, which are typical of wet winding. Hoop layers are wound twice (of double thickness), offsetting the winding path with half the band width of rotation to stagger band crossover locations.

Within the tube body fiber angle of a layer is held constant. Outboard the tube body the fiber angle is transitioned to 90 deg and redirected back symmetrically (reversed) to make a circuit. Hoop layers are reversed in trap grooves (i.e. continuous) of the pattern set. Reversing axial layers requires pin rings<sup>7</sup> (cut fibers).

Since hoop windings are near 90 deg, its path may be reversed in a reasonable distance by gradually increasing fiber angle as the winding band approaches the trap groove, at a rate within the limits of friction.

For optimum traplock performance, the fiber angle of axial layers must be maintained across the trap groove. To reverse axial windings, pin rings installed outside the traplock are used to hook the winding band. After finishing an axial layer, a local buildup of 90 deg windings is wound in the trap grooves (both ends). These trap fills compact the groove, cross-reinforce the axial layers, and give the trap circumferential stiffness to resist dilation when the MCI is loaded in tension. Once tied down by the trap fill, axial windings are cut free from pin rings and offal material removed. For added MCI axial strength, plies of unidirectional mat (0 deg) are wound into the MCI area.

The process of winding, applying of mat, and trap fills associated with a pattern set is repeated for each trap pair. After all six pattern sets are complete, additional hoop windings are applied over the MCI to reinforce the traplock.

### **Sacrificial Glass Top Layer**

After finishing the structural composite, the outer layer of HNBR is added, and a layer of Owens Corning Advantex E-glass fiber (a boron-free and corrosion resistant formulation) is wound overtop. Glass fiber is a very durable and inexpensive material and makes an excellent outer scuff layer for protection against handling damage (scratches and abrasion). After winding the glass fiber top layer, the part is cured in an oven at 149 °C (300 °F). The final step is to apply a polyurethane topcoat over the composite to provide UV protection and as a marine growth inhibitor.

---

<sup>7</sup> Pin rings are a winding aid (installed at both ends of the part) with radially protruding pins that are used to hook the winding band.



Nominal properties of a finished riser joint are listed in Table 7-10.

**Table 7-10: Riser Joint Summary**

	SI	USC
Joint Length	22,9 m	75 ft
Tube Body Diameter	665,5 mm	26.20 inch
Pipe Thickness	25,4 mm	1.00 inch
Steel Weight + Coupling Hardware	14 047 kg	30,969 lb
Composite Thickness	53,3 mm	2.10 inch
Composite Weight	3 362 kg	7,411 lb
Joint Weight	17 409 kg	38,380 lb
Averaged Weight	761,5 kg/m	511.7 lb/ft
Averaged Wet Weight (without buoyancy)	580,1 kg/m	389.8 lb/ft
Extensional Stiffness, E-A <sup>1</sup>	1,20 10 <sup>10</sup> N	2.70 10 <sup>9</sup> lbf
Bending Stiffness, E-I <sup>1</sup>	5,19 10 <sup>8</sup> N-m <sup>2</sup>	1.81 10 <sup>11</sup> lbf-inch <sup>2</sup>

<sup>1</sup> Tube body section

## Autofrettage

An essential part of this composite riser design is pre-stressing by autofrettage. Autofrettage is a procedure performed by the manufacturer in which a joint is pressurized to a stress level greater than the yield strength of the steel, expanding the pipe inside the composite plastically. After pressure is released, there remains a permanent interference fit between the steel pipe and composite; leaving the composite fibers in tension and the steel in residual compression. The autofrettage pressure is selected such that the stress created is greater than will be experienced in service (e.g. field pressure test or a gas kick). This ensures even the most extreme loadings have a completely elastic material response.

Autofrettage is safe and a common manufacturing technique to improve the efficiency and reliability of composite over-wrapped pressure vessels (COPV). There are two key benefits from autofrettage for this riser design. First it improves utilization of the steel by setting the condition of stress for normal service loads near its compressive yield strength. In the event of a gas kick, the elastic range to resolve the load is approximately double. A design without autofrettage would require considerably more composite (stiffness) to yield the same stress. The second reason for autofrettage is improved fatigue performance. Under normal service loads the steel hoop stress is in compression and the axial stress is near zero.

## Weight and Estimated Cost

The dry weight of composite and steel is compared in Figure 7-1 for a 22,9 m (75 ft) joint having a total weight of 17 409 kg (38,380 lb). The comparable weight of a conventional X80 joint is estimated at 31 319 kg (69,046 lb), having a 84,3 mm (3.32 inch) wall and requiring 37,06 MN (8,331 kipf) of top-tension. This figure is based on a design sized using API RP 2RD allowable stress criteria for a top joint during a gas kick (ref. section 8,  $C_f=1.20$ ). Weight savings made possible by composites is 44.4% dry and 51.3% wet. Required top-tension is reduced 63.3%.

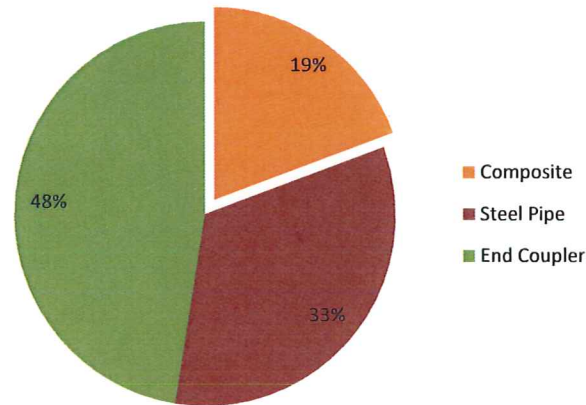


Figure 7-1: Joint Weight Breakdown

The estimated cost for a 22,9 m (75 ft) joint is 375 M USD (\$5,000/ft). A breakdown by primary component and operations is illustrated in Figure 7-2. These figures are based on budgetary quotes for the steel assembly and typical production rates for the composite (materials and winding process). It is important to note the coupler size has a profound impact on both weight and cost, and for this reason other connector types may be considered.

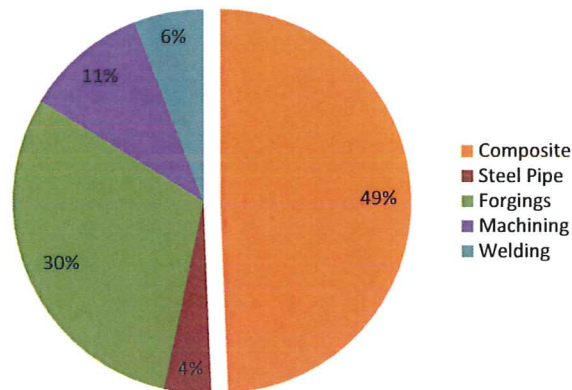


Figure 7-2: Estimated Joint Cost

- API 5L Grade X80M PSL2 DSAW Pipe	15 M USD
- Modified ASTM A 182 grade F22 Forgings	114 M USD
- Machining of End Couplers	39 M USD
- Welding and Grinding Steel Assembly	22 M USD
- Composite (material, labor, overhead, profit)	185 M USD

## 8. Design and Analysis

The design of a composite riser is more complex than for conventional risers, with many failure mechanisms and where local effects are crucial to most failure modes. It is not possible to establish acceptance criteria on a global level for all failure modes; therefore, an iterative global-local procedure has been used to design and analyze the riser. Global load effects (i.e. tension, pressure, and bending), as determined by global analysis, serve as boundary conditions for local analysis. Local load effects are then evaluated using local design criteria.

### Riser Configuration

The base case for design is a dry tree drilling riser deployed from a generic spar platform in 3 048 m (10,000 ft) of water, and having a pressure rating of 103,4 MPa (15,000 psi). A stack-up diagram of the riser system is shown in Figure 8-1 with elevations and component weights listed in Table 8-1.

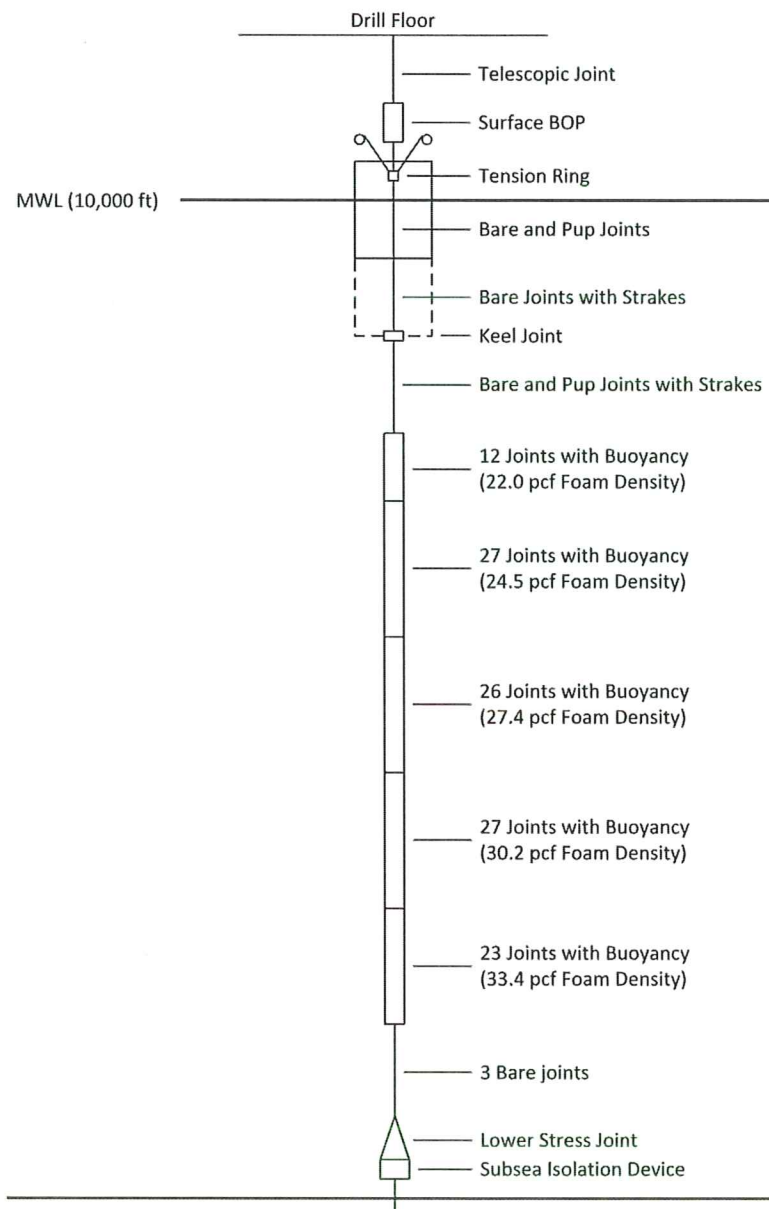


Figure 8-1: Riser Stack-up Diagram

### **Spar Structure**

The spar is a truss design, with a 167,6 m (550 ft) draft, of which 61,0 m (200 ft) is comprised of hard tank. Riser centralizers are located at 76,2 m (250 ft), 106,7 m (350 ft), and 167,6 m (550 ft, keel joint) below the water line.

### **Surface Components**

Surface components consists of a tension joint/ring, surface blowout preventer (SBOP), and the telescopic joint; connecting the riser to the diverter system at the drill floor. Approximate stroke length of the telescopic joint is 10,8 m (35.4 ft). Estimated weight of the SBOP is 95,3 t (210 kip).

### **Drilling Riser**

The drilling riser is made up of 22,9 m (75 ft) joints having properties as listed in Table 7-10. The riser system is configured without choke and kill or auxiliary lines. To address the potential for vortex induced vibration (VIV), suppression strakes are assumed on all bare joints below the hard tank.

### **Buoyancy**

To meet the targeted top-tension, riser buoyancy is necessary. Four 4,6 m (180 inch) by 1,42 m (56 inch) diameter syntactic foam modules are installed per buoyed joint. Foam density is varied with depth using data provided by Cumming Corporation for C-FLOAT ULF material. Foam utilization was estimated at 93 %. Total lift from buoyancy is 13,5 MN (3,028 kipf) providing an average compensation of 90 % for buoyed joints. The weight of stop collars and assembly hardware has been included.

The required riser top-tension with buoyancy is 13,61 MN (3,060 kipf) using 16 ppg mud and a 1.3 tension factor.

### **Lower Stress Joint and Keel Joint**

To get an accurate representation of bending at the top and bottom of the riser, a preliminary tapered steel joint for at the keel and for the lower stress joint were designed by Kenneth Bhalla of Stress Engineering Services.

### **Subsea Components**

At the sea floor, a VetcoGray MS-700 wellhead system is connected to 36-inch conductor casing. Wellhead stick-up height to the top of the high-pressure housing is 3 m (10 ft). To the wellhead, a 117,9 t (260 kip) subsea isolation device (SID) is installed. The lower stress joint is attached to the SID by an external tieback connector having properties based on a VetcoGray SHD-H4.

Without auxiliary lines supported by the riser, subsea equipment is expected to be operated by a remote operated vehicle (ROV) or other temporary system.



**Table 8-1: Riser Stack-up Listing**

	SI					USC				
	Elevation	Weight, t				Elevation	Weight, kip			
	m	Dry	Wet	Lift	Net	ft	Dry	Wet	Lift	Net
Conductor Casing	0	0,9	0,8		0,8	0	2	2		2
Low Pressure Housing	1,1	1,9	1,7		1,7	3,7	4	4		4
High Pressure Housing	2,1	2,9	2,5		2,5	7	6	6		6
Subsea Isolation Device	3,0	117,9	102,5		102,5	10	260	226		226
Tie-back Connector	9,3	13,0	11,3		11,3	31	29	25		25
Lower Stress Joint	10,4	26,1	22,7		22,7	34	57	50		50
Bare Riser Joints	30,8	52,2	39,8		39,8	101	115	88		88
Buoyed Joints (33.4 pcf)	99	400,0	305,0	-233,3	71,6	326	883	672	-514	158
Buoyed Joints (30.2 pcf)	625	470,0	358,0	-302,8	55,2	2,051	1,036	789	-668	122
Buoyed Joints (27.4 pcf)	1 242	452,6	344,7	-315,9	28,9	4,076	998	760	-696	64
Buoyed Joints (24.5 pcf)	1 837	470,0	358,0	-354,2	3,8	6,026	1,036	789	-781	8
Buoyed Joints (22.0 pcf)	2 454	208,9	159,1	-167,4	-8,3	8,051	461	351	-369	-18
Bare Joints with Strakes	2 728	107,7	78,4		78,4	8,951	237	173		173
Keel Joint	2 862	43,7	38,0		38,0	9,391	96	84		84
Bare Joints with Strakes	2 898	55,0	40,0		40,0	9,509	121	88		88
Bare Joints (below MWL)	2 967	61,7	47,0		47,0	9,734	136	104		104
Bare Joints (above MWL)	3 048	5,0			5,0	10,000	11			11
Tension Joint (below ring)	3 054	10,6			10,6	10,021	23			23
Tension Joint (above ring)	3 060	6,8			6,8	10,040	15			15
Surface BOP	3 062	95,3			95,3	10,046	210			210
Telescopic Joint	3 069					10,070				
Drill Floor	3 080					10,105				

## Global Analysis

Global analysis of the presented riser system was performed by Kenneth Bhalla of Stress Engineering Services using an internally developed frequency domain analysis program DERP. The following design load cases were identified by the project working committee for evaluation:

- Field Pressure Test (FPT): MAOP shut-in at SBOP with 64 pcf seawater
- Normal Operating (NO): 16 ppg drilling mud
- Hydrostatic Collapse (HC): Entire column filled with seawater
- Gas Kick (GK): MAOP shut-in at SBOP with 50 % gas cut mud (8 ppg)
- Mooring Failure (MF): Normal Operating with a greater mean offset

The maximum allowable operating pressure (MAOP) is the rated pressure of the SBOP (103,4 MPa, 15,000 psi).

The collapse case is making up for lost circulation by pumping seawater into the riser. In the extreme condition the entire riser column is filled with seawater, in which case the cross-section is in equilibrium. While the riser is not at risk of collapsing, it is the load case resulting in the most compressive axial stress.

Tension and internal pressure profiles for each load case are listed in Table 8-2 and Table 8-3 respectively.

Drag loads due to current were not explicitly considered in the analysis.

**Table 8-2: Riser Tension Profiles**

	SI				USC			
	Elevation	Tension, MN			Elevation	Tension, kipf		
	m	FPT/HC	NO/MF	GK	ft	FPT/HC	NO/MF	GK
Conductor Casing	0	0,11	1,72	-0,01	0	26	386	-1
Low Pressure Housing	1,1	0,12	1,73	0,00	3.7	28	389	1
High Pressure Housing	2,1	0,14	1,75	0,02	7	31	393	4
Subsea Isolation Device	3,0	0,16	1,77	0,04	10	37	399	10
Tie-back Connector	9,3	1,17	2,79	1,05	31	263	627	236
Lower Stress Joint	10,4	1,28	2,90	1,16	34	288	652	260
Bare Riser Joints	30,8	1,50	3,16	1,38	101	338	710	310
Buoyed Joints (33.4 pcf)	99	1,89	3,67	1,76	326	425	825	395
Buoyed Joints (30.2 pcf)	625	2,59	5,31	2,39	2,051	583	1,193	538
Buoyed Joints (27.4 pcf)	1 242	3,14	6,94	2,85	4,076	705	1,561	641
Buoyed Joints (24.5 pcf)	1 837	3,42	8,28	3,06	6,026	769	1,861	687
Buoyed Joints (22.0 pcf)	2 454	3,46	9,41	3,01	8,051	777	2,116	677
Bare Joints with Strakes	2 728	3,37	9,82	2,89	8,951	759	2,207	651
Keel Joint	2 862	4,14	10,82	3,64	9,391	931	2,433	819
Bare Joints with Strakes	2 898	4,52	11,26	4,01	9,509	1,015	2,531	902
Bare Joints (below MWL)	2 967	4,91	11,77	4,40	9,734	1,103	2,647	988
Bare Joints (above MWL)	3 048	5,37	12,38	4,85	10,000	1,207	2,782	1,089
Tension Joint (below ring)	3 054	5,43	12,45	4,91	10,021	1,221	2,799	1,103
Tension Joint (above ring)	3 060	5,55	12,58	5,02	10,040	1,247	2,827	1,129
Surface BOP	3 062	5,62	12,65	5,09	10,046	1,263	2,844	1,145
Telescopic Joint	3 069	6,57	13,61	6,04	10,070	1,476	3,060	1,358
Drill Floor	3 080				10,105			

<sup>1</sup> 1.3 tension factor for all load cases

**Table 8-3: Riser Internal Pressure Profiles**

	SI					USC				
	Elevation	Pressure, MPa				Elevation	Pressure, psi			
	m	FPT	NO/MF	HC	GK	ft	FPT	NO/MF	HC	GK
Conductor Casing	0	134,20	57,91	30,97	132,21	0	19,465	8,399	4,491	19,175
Low Pressure Housing	1,1	134,19	57,89	30,95	132,19	3.7	19,463	8,396	4,489	19,173
High Pressure Housing	2,1	134,18	57,87	30,94	132,19	7	19,462	8,393	4,488	19,172
Subsea Isolation Device	3,0	134,17	57,85	30,93	132,18	10	19,460	8,391	4,487	19,171
Tie-back Connector	9,3	134,11	57,73	30,87	132,12	31	19,451	8,374	4,478	19,162
Lower Stress Joint	10,4	134,10	57,71	30,86	132,11	34	19,450	8,371	4,476	19,161
Bare Riser Joints	30,8	133,89	57,33	30,66	131,92	101	19,420	8,315	4,446	19,133
Buoyed Joints (33.4 pcf)	99	133,21	56,04	29,97	131,27	326	19,320	8,128	4,346	19,039
Buoyed Joints (30.2 pcf)	625	127,92	46,15	24,68	126,33	2,051	18,553	6,694	3,580	18,322
Buoyed Joints (27.4 pcf)	1 242	121,71	34,55	18,47	120,53	4,076	17,653	5,011	2,680	17,481
Buoyed Joints (24.5 pcf)	1 837	115,74	23,38	12,50	144,94	6,026	16,786	3,390	1,813	16,670
Buoyed Joints (22.0 pcf)	2 454	109,53	11,77	6,29	109,14	8,051	15,886	1,707	913	15,829
Bare Joints with Strakes	2 728	106,78	6,61	3,54	106,56	8,951	15,486	959	513	15,455
Keel Joint	2 862	105,43	4,09	2,19	105,30	9,391	15,291	593	317	15,272
Bare Joints with Strakes	2 898	105,07	3,42	1,83	104,96	9,509	15,238	495	265	15,223
Bare Joints (below MWL)	2 967	104,38	2,13	1,14	104,31	9,734	15,138	308	165	15,129
Bare Joints (above MWL)	3 048	103,56	0,60	0,32	103,55	10,000	15,020	87	47	15,019
Tension Joint (below ring)	3 054	103,50	0,48	0,26	103,49	10,021	15,011	70	38	15,010
Tension Joint (above ring)	3 060	103,44	0,38	0,20	103,44	10,040	15,003	54	29	15,002
Surface BOP	3 062	103,42	0,34	0,18	103,42	10,046	15,000	49	26	15,000
Telescopic Joint	3 069		0,20	0,11		10,070		29	16	
Drill Floor	3 080		0	0		10,105		0	0	

### Sea State

A 100-year hurricane storm condition was assumed in evaluating all design load cases (FPT, NO, HC, GK, MF). Global analysis was performed using metocean data and motion response amplitude operators (RAO) provided by industry participants for Horn Mountain.

Characteristic parameters for modeling sea conditions:

- Significant wave height (Hs) of 14,2 m (46.59 ft)
- Peak wave period (Tp) of 15.4 seconds
- Wave spectral peakedness factor (gamma) of 2.4

Of twelve wave headings, the RAO of the worst case was selected. Two mean offset conditions were examined. A 1.9 % offset (of water depth) for all load cases except the mooring failure survival case, which was at 7.6 % offset.

Fatigue was evaluated assuming the same 100-year hurricane storm condition (i.e. extreme loads).



### Design Load Case Matrix

Modeling composite risers is complex and requires tedious post-processing to resolve global load effects to local design criteria. With much of local analysis being performed manually, to analyze the full length of the riser is at this time prohibitive. To scope the analysis to a manageable level, the locations of highest tension (topmost joint) and highest pressure differential (bottommost joint) were examined. These are also locations of highest bending.

At the time global analysis was performed it was assumed all standard joints would be of the composite-reinforced design. It was later decided joints above the keel should be steel to address concerns for fire safety and the impact of wear from centralizers. Therefore, top and bottom locations referred to in local analysis are immediately below the keel joint and above the lower stress joint. Global analysis was not updated to reflect this change; however, the error is not expected to have a significant impact on results.

Global load effects at top and bottom locations for each design load case are listed in Table 8-4 and Table 8-5. Tension and internal pressure are according to Table 8-2 and Table 8-3. External pressure is based on 64 pcf seawater and depth relative to the mean water line (MWL). Bending moment is from the global analysis solution and represents the most probable maximum in 1 000 waves (approximate duration of a three hour storm).

**Table 8-4: Design Load Case Matrix**

Load Case	Joint Position <sup>1</sup>	SI				USC			
		Tension MN <sup>2</sup>	Pressure, MPa		Bending kN-m	Tension kipf <sup>2</sup>	Pressure, psi		Bending kipf-ft
			Internal	External			Internal	External	
Autofrettage (AF) <sup>8</sup>	NA	0	137,90	0	0	0	20,000	0	0
Factory Acceptance Test (FAT) <sup>3 8</sup>		0	129,28	0	0	0	18,750	0	0
Field Pressure Test <sup>4 5 9 10 11</sup>	T	4,14	105,43	1,87	1 308	931	15,291	271	965
	B	1,50	133,89	30,33	652	338	19,420	4,400	481
Normal Operating <sup>6 9 10 11</sup>	T	10,82	4,09	1,87	997	2,433	593	271	735
	B	3,16	57,33	30,33	681	710	8,315	4,400	502
Hydrostatic Collapse <sup>4 9 10 11</sup>	T	4,14	2,19	1,87	1 308	931	317	271	965
	B	1,50	30,66	30,33	652	338	4,446	4,400	481
Gas Kick <sup>5 7 9 10 11</sup>	T	3,64	105,30	1,87	1 335	819	15,272	271	985
	B	1,38	131,92	30,33	639	310	19,133	4,400	471
Mooring Failure <sup>6 9 10 12</sup>	T	10,82	4,09	1,87	1 352	2,433	593	271	997
	B	3,16	57,33	30,33	2 203	710	8,315	4,400	1,625

<sup>1</sup> T-top (keel joint), B-bottom (lower stress joint)

<sup>2</sup> 1.3 tension factor

<sup>3</sup> FAT 125 % of MAOP

<sup>4</sup> Riser filled with 64 pcf seawater

<sup>5</sup> 15,000 psi at SBOP

<sup>6</sup> Riser filled with 16 ppg mud

<sup>7</sup> 50 % gas-cut mud

<sup>8</sup> Evaluated at 21 °C (70 °F)

<sup>9</sup> Evaluated at 82 °C (180 °F)

<sup>10</sup> Hs=14,2 m (46.59 ft), Tp=15.4 seconds, Gamma=2.4

<sup>11</sup> 1.9 % mean offset

<sup>12</sup> 7.6 % mean offset

**Table 8-5: Load Category, Frequency, and Duration**

Load Case	Load Category	C <sub>f</sub>	Number of Events (20 year life)	Event Duration hr
Autofrettage	NA		1	.50
Factory Acceptance Test	Test	1.35	1	.25
Field Pressure Test	Test	1.35	80	1
Normal Operating	Operating	1.00	Infinite	175200
Hydrostatic Collapse	Extreme	1.20	2	72
Gas Kick	Extreme	1.20	2	72
Mooring Failure	Survival	1.50	1	3



The load steps used in the local analysis model and the order in which they are applied are listed in Figure 8-2. Load steps 7 and 9 are the design load cases of interest. Each load step is solved sequentially (from step 1 to 9), building a load history consistent with what a riser joint would experience prior to each design load case.

Load Step	Description
1	Post Cure Cooldown
2	Autofrettage
3	Post AF Condition
4	Factory Acceptance Test
5	Post FAT Condition
6	Connected with Seawater
7	Field Pressure Test (FPT)
8	Normal Service
9	Normal Operating (NO)
9	Hydrostatic Collapse (HC)
9	Gas Kick (GK)
9	Mooring Failure (MF)

**Figure 8-2: Load Sequencing**

Load steps 1-5 are performed at the factory by the manufacturer. Load step 1 is simply a temperature change from the oven temperature used to cure the epoxy to ambient. This step is necessary prior to autofrettage to create the post cure radial gap between steel and composite that occurs during cooldown (CTE).

Every joint prior to leaving the factory is subject to both an autofrettage and a factory acceptance test pressure cycle. Autofrettage is a pre-stressing operation used to induce residual compressive stresses in the steel pipe by expanding it inside the composite plastically (ref. section 7). The factory acceptance test is a quality assurance requirement to demonstrate integrity prior to releasing a joint for service.

After the riser has been run and connected (step 6), a field pressure test is performed with seawater to verify the integrity of seals between joints (step 7). When complete, seawater is displaced with mud and the drilling process begins (step 8). Load steps 6 and 8 are connected and tensioned but without bending.

Load steps 7 and 9 are the design load cases, evaluated with bending of a 100-year hurricane storm. Load step 8 is therefore normal service after having first experience field pressure test in extreme conditions. Since loads on the riser are location dependent, once it has been connected (step 6) the load histories for top and bottom joints are unique and tracked separately.

Fatigue was evaluated considering the cumulative effects of autofrettage and factory acceptance test (steps 1-5); the field pressure test (step 7), gas kick, and normal operating design load cases (i.e. extreme loads), for the cycle counts listed in Table 8-5 representing a 20 year service life.

## Local Analysis

Analysis of the riser joint was performed by Lincoln Composites using a general purpose finite element (FE) code and internally developed pre and post-processing software for the load cases listed in Table 8-4.

### Analytical Model

The riser joint was analyzed using the commercial FE code ANSYS Mechanical APDL. Composite and steel were defined as separate components interacting through surface contact at the interface.

The composite was modeled as a layered structure with each wound layer, trap fill, and mat ply represented by a discrete layer of elements. Mesh density was controlled to limit element aspect ratio to approximately 4:1. For a typical layer thickness of 0,76 mm (.030 inch), an element should be 3,05 mm (0.120 inch) or less in length. Considering the number of composite layers, the joint length, and element size restrictions; to model a full joint in 3-D is prohibitive. To keep the FE model within a manageable size an axisymmetric analysis with length symmetry was necessary. An illustration of the FE mesh is shown in Figure 8-3. The tube body is three diameters in length.

Since the model must support non-linear behavior, harmonic elements allowing non-axisymmetric loadings were not an available option. Instead, bending moment was represented as an additional axial end force having a wall stress equivalent to the stress of bending based on beam equations. Therefore, each load step (Figure 8-2), for top and bottom locations, has two separate solutions: one for each side relative to the neutral axis. The two solutions are marked in results by +M (positive end force, tension side) and -M (negative end force, compression side).

The element type used for both composite and steel is the PLANE42. This 4-node 2-D structural element is unique in that it supports orthotropic material property inputs relative to the element (i-j) side. This feature allows layer properties to be defined relative to a meridional coordinate system, consistent with filament-wound construction.

Element layers are modeled specially orthotropic with each element assigned a fiber angle and thickness according to the winding path at its location. Material constants are derived by considering each element as a symmetric sub-laminate of the given fiber angle (i.e.  $[\pm\theta]_s$ ). This involves averaging the fourth-order tensor transformation of the composite unidirectional stiffness matrix into the meridional coordinate system. The unidirectional stiffness matrix is based on 3-D constitutive equations and micromechanics expressions using fiber and matrix properties.

During autofrettage, micro-crazing (microscopic cracks) is expected in the matrix between fibers. This is normal and accounted for in analysis by reducing unidirectional properties transverse to fibers to a very small value.

The steel was modeled with multi-linear kinematic hardening (KINH). The stress-strain curve for pipe is based on mechanical testing of pipe purchased for prototyping. The plastic portion of the curve was offset to the minimum yield strength. The same data was used for the end coupler except offset for grade F22 steel. Pipe diameter and MCI geometry were modeled at nominal dimensions with an inside bore diameter leaving the minimum allowable pipe wall thickness per API 5L. The end coupler flange was designed by Allen Fox of Stress Engineering Services and analyzed separately. For this model it is not the focus of analysis and was fully defeatured.

The interface between steel and composite was modeled with a CONTA171 and TARGE169 contact pair configured to provide behavior consistent with an unbonded interface.

For boundary conditions, the UY nodal DOFs at the open end of the tube body were set to zero (length symmetry) and coupled (CP) at the flange. Tension, pressure end force, and bending force are applied to the flange in the FY direction. Internal pressure was applied to the inside bore. External pressure was applied to all outside surfaces. The effects CTE and post cure cooldown were included by setting the environment temperature (TUNIF) relative to the stress free temperature (TREF) of cured composite.

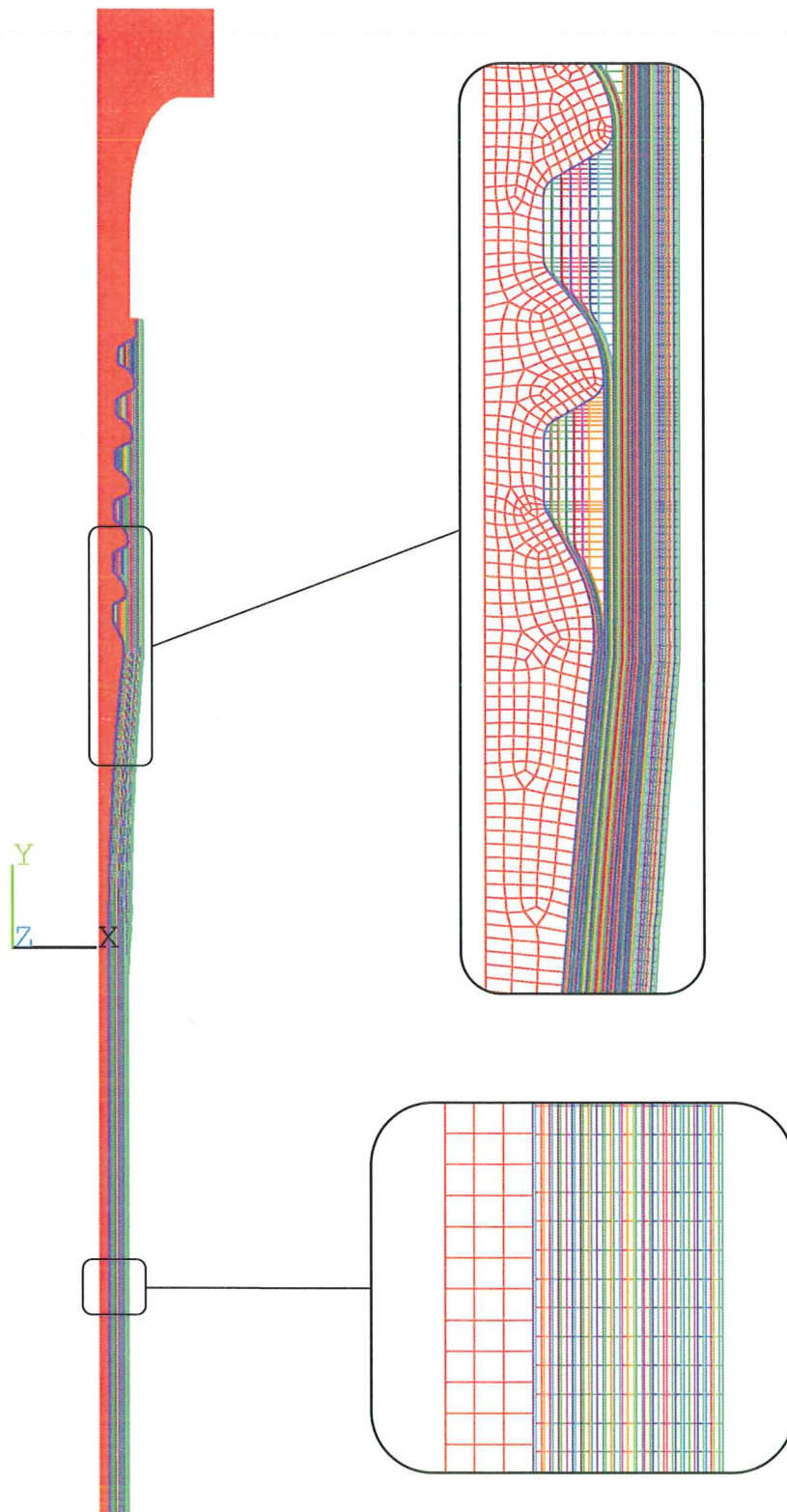


Figure 8-3: Local Analysis FE Model



### Design Fiber Strength

The allowable composite fiber stress for design is based on testing performed under the NIST-ATP project, published literature, and experience with similarly designed products having extensive field history.

The mean tensile strength of carbon fiber is 3 103 MPa (450 ksi) based on burst results under the NIST-ATP project. This is 60 % less than the typical value reported by Toray for T700SC fiber. The ratio of apparent strength, as determined by post failure analysis of test results, to its certified strength is called translation; a factor accounting for process related fiber damage, stress concentrations, and laminate defects that cannot be readily modeled.

In composite design, there are two main fiber failure mechanisms to be considered: static fatigue (stress rupture) and cycle fatigue. Different fiber types (carbon, glass, or aramid) have a different allowable stress depending on its unique susceptibility to failure. These allowables are expressed as a stress ratio – mean strength to working stress.

Stress rupture is well characterized by E.Y. Robinson<sup>8</sup>. The expected long term static strength of carbon fiber for a 20 year sustained load is 52.2 % of its mean strength, or a stress ratio (SR) of 1.92. This value is based on a design curve associated with a  $10^{-5}$  probability of failure. Testing under the NIST-ATP project confirmed Robinson's data.

For autofrettage and the factory acceptance test pressure cycle, the allowed fiber stress is 1 620 MPa (234.9 ksi). This is a conservative value considering time at these pressures is less than one hour. This value is also appropriate for field pressure test and gas kick load cases; however, a more restrictive allowable is applied for cyclic fatigue.

The cyclic fatigue performance of composites is unique to every design and is limited less by material capability and more by the skill of the designer and the quality of construction. The fatigue qualification approach common to composite over-wrapped pressure vessels (COPV) is to demonstrate a design life at least three times greater than the rated number of service cycles. Through experience, a 2.25 SR is considered sufficient for carbon fiber in applications of full-range pressure cycles with a design life of 50 000 cycles. The corresponding allowable fiber stress is 1 379 MPa (200 ksi). This is a conservative value considering the limited number of high pressure events.

There is limited information on carbon fiber strength in compression. Prior composite riser design work has been based on an allowable compressive fiber stress of 689,5 MPa (100 ksi). The same was used for this design.

### Autofrettage and Factory Acceptance Test

The solution to load steps 1-5 (ref. Figure 8-2) are illustrated in Figure 8-4 through Figure 8-11. Stresses are in USC units of ksi. Figure 8-4 and Figure 8-5 are stress-strain plots illustrating material behavior in the tube body for steel pipe and composite fibers during the autofrettage and factory acceptance test pressure cycles.

Load step 1 begins with the steel pipe pulled away from composite and under slight axial tension (CTE and post cure cooldown). During autofrettage (step 2) the pipe is expanded to 1.3 % strain. The composite fiber having the highest stress is in the inside hoop layer. The highest stressed axial fiber is 60 % of the hoop stress (A/H ratio). After pressure has been removed (step 3), the composite fibers are in tension and the steel pipe is in compression. The stress of both materials at factory acceptance test pressure (step 4) are less than they were at autofrettage, and fully recover elastically to the post autofrettage condition as pressure is released (step 5).

Composite fiber stresses at the MCI during autofrettage are plotted in Figure 8-10 for hoop layers and Figure 8-11 for axial layers. The horizontal axis is element location relative to the open end of the tube body. Fiber stresses are constant in the tube body and decrease at the MCI. A key advantage of a traplock approach over other MCI concepts is that it can be designed stronger than the tube body, eliminating it as the design limiting failure mode.

---

<sup>8</sup> E.Y. Robinson, Design Prediction of Long-Term Stress Rupture Service of Composite Pressure Vessels, Aerospace Report No. ATR-92(2743)-1, The Aerospace Corporation, 1991

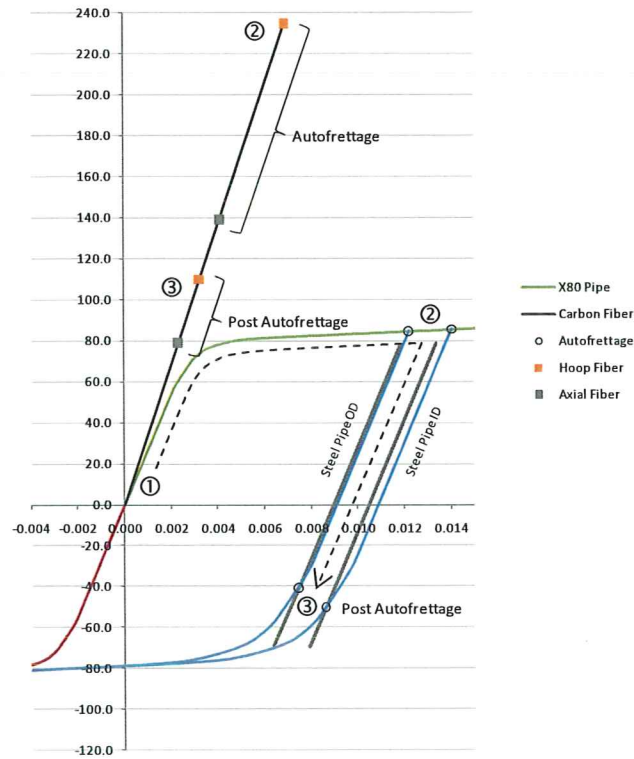


Figure 8-4: Autofrettage – Tube Body

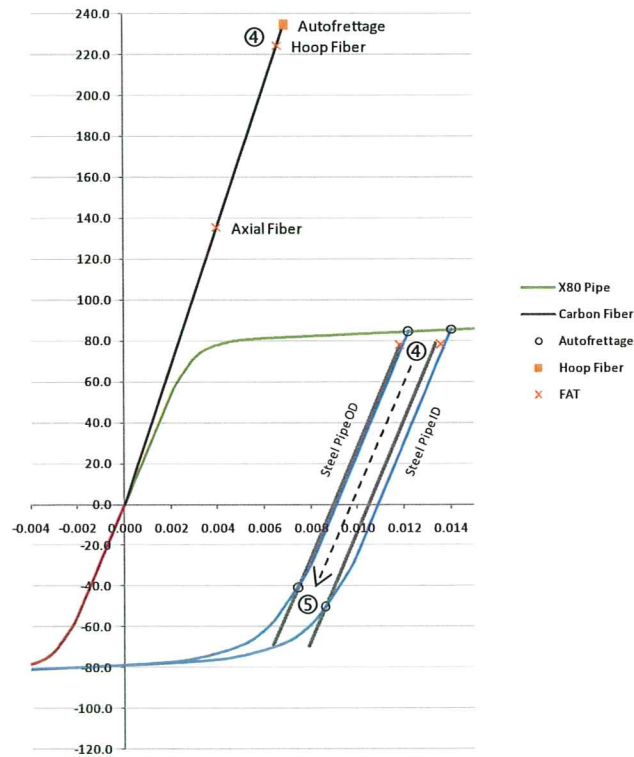


Figure 8-5: Factory Acceptance Test – Tube Body

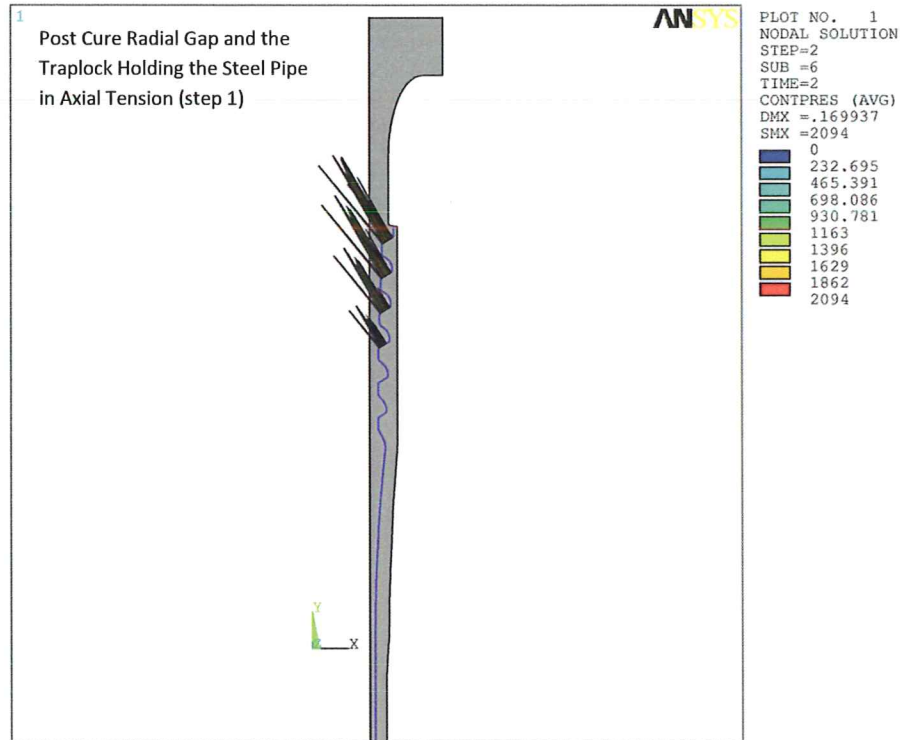


Figure 8-6: Post Cure Interface Pressure

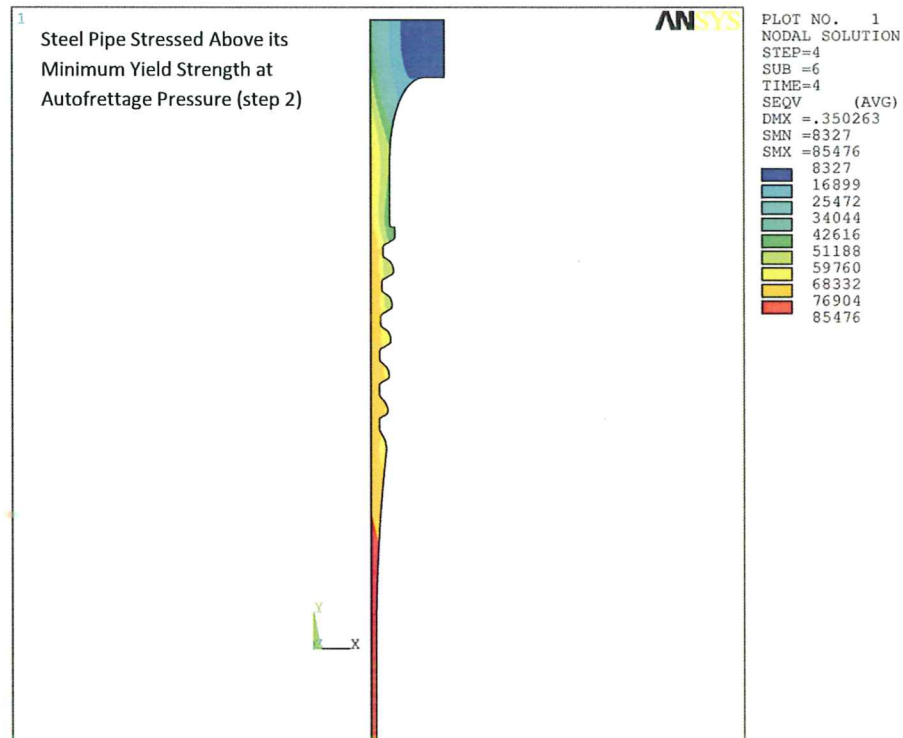


Figure 8-7: Autofrettage – Steel Stress

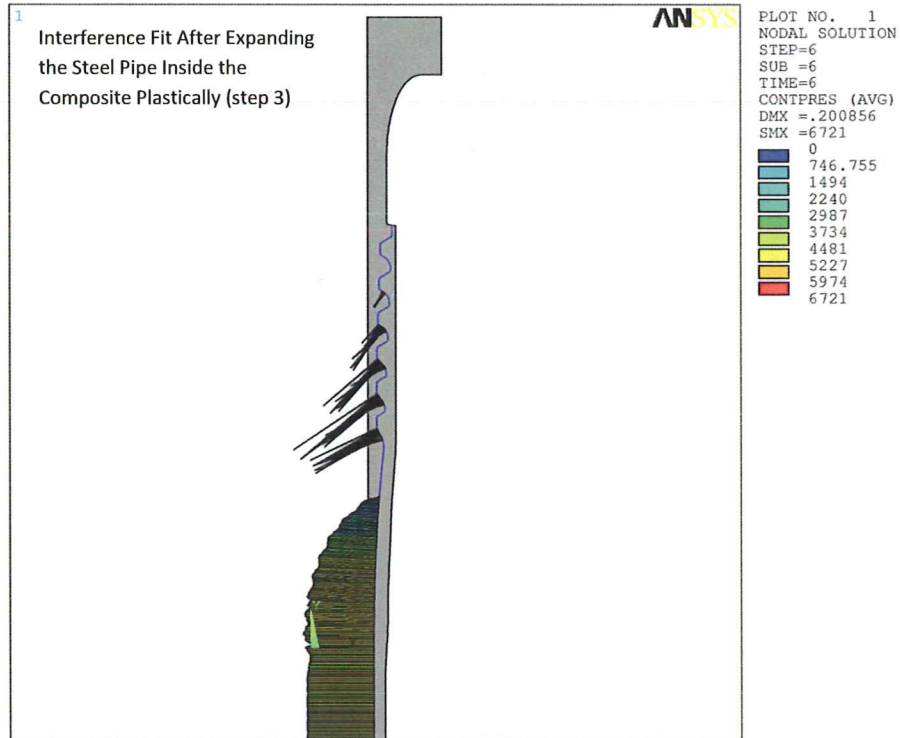


Figure 8-8: Post Autofrettage Interface Pressure

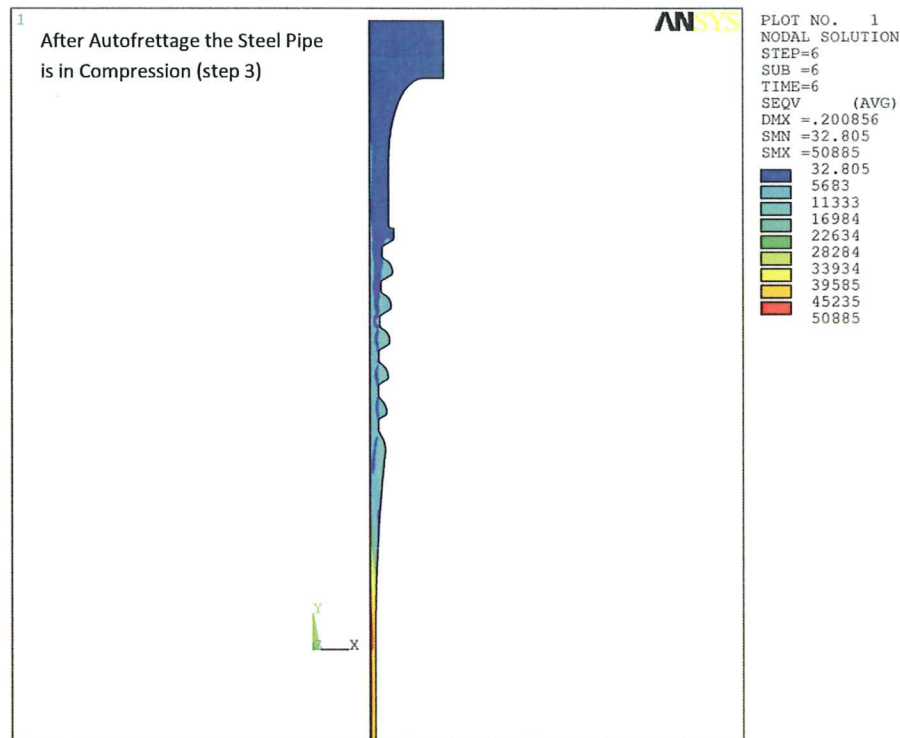


Figure 8-9: Post Autofrettage – Steel Stress



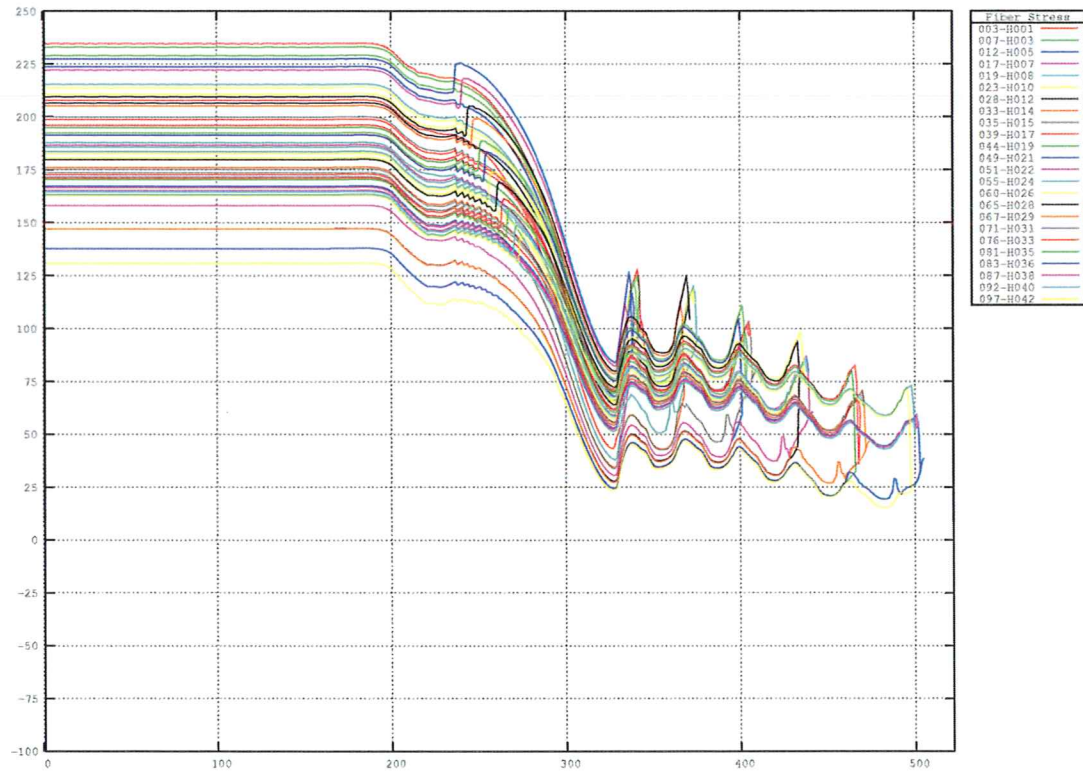


Figure 8-10: Autofrettage – Hoop Fiber Stress

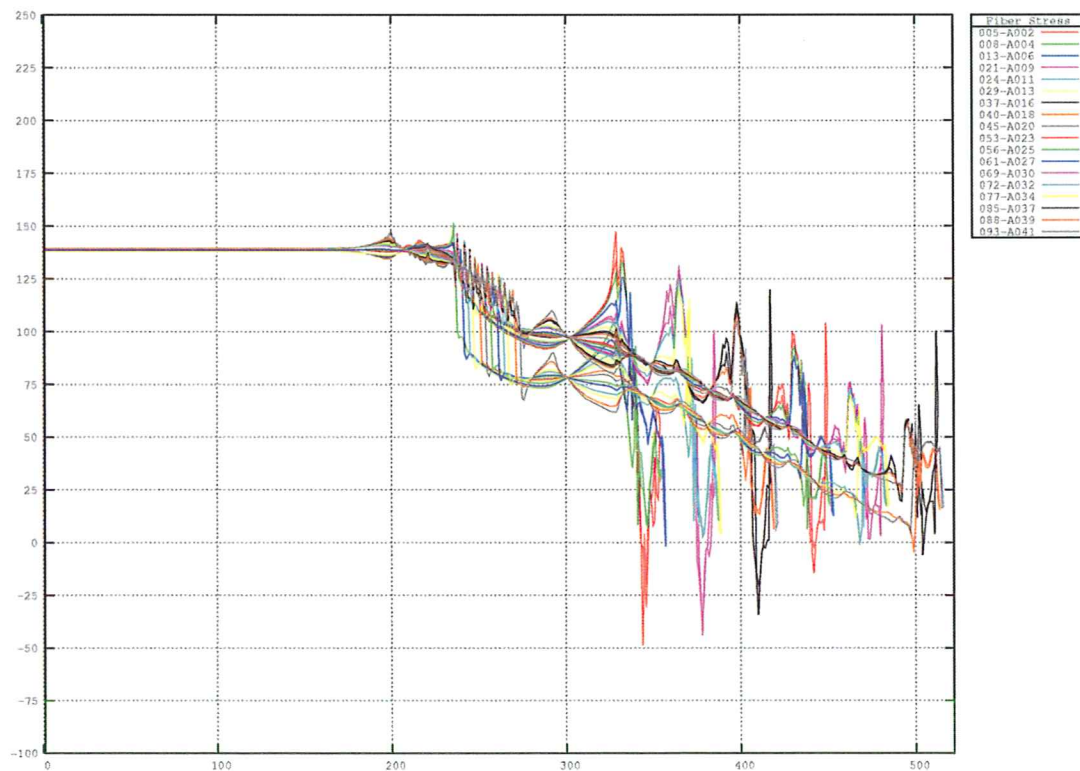


Figure 8-11: Autofrettage - Axial Fiber Stress



### Design Load Cases

The tube body solution to each of the design load cases is plotted in Figure 8-12 through Figure 8-16. Stresses are in USC units of ksi. These stresses are also listed in Table 8-6 and Table 8-8 with their corresponding allowables. The reported hoop and axial composite fiber stresses are the peak values occurring in respective layers of the laminate. As reference information, hoop and axial components of the steel pipe stress are provided in Table 8-9.

Allowable stresses for the steel pipe based on API RP 2RD are given in Table 8-7 for each of the design load cases. These values were not used as design criteria and only presented in this report to compare results to conventional allowables. Stresses failing to meet 2RD allowable stresses are marked in red and underlined, and show utilization greater than 100 %. The same value was applied to both tensile and compressive stresses assuming strength in the two directions are equal.

The requirement for limiting stress in the steel was to operate elastically (to not exceed the stress at autofrettage). Although this is different from the criteria of 2RD, it is consistent in that both limit stress to the proportional range of the material (i.e. to roughly two-thirds the 0.2% offset yield strength).

The highest stress a riser joint will ever experience occurs during autofrettage. The results for autofrettage have already been presented. The highest stress the riser will see once in service occurs at the top joint during a field pressure test or gas kick (+M) (the two design load cases are nearly equivalent). For both design load cases, the peak stress is 30 % less in the composite fibers and 10 % less in the steel pipe than during autofrettage relative to the stresses of normal service.

The most compressive stress in the composite fibers occurs at the top joint for the hydrostatic collapse design load case (-M). Composite fiber stresses for this case are plotted in Figure 8-18 for hoop layers and Figure 8-19 for axial layers. Stresses are in USC units of ksi. The most compressive stress is within the 689,5 MPa (100 ksi) allowable.

The most compressive stress in the steel pipe occurs at the top joint for the mooring failure design load case (+M). Figure 8-17 is a contour plot of steel pipe and end coupler stresses for this case. Stresses are in USC units of ksi.

Between autofrettage (the most tensile load condition) and the hydrostatic collapse and mooring failure design load cases (the most compressive load conditions) the full range of stresses have been bounded.

Stress in the steel pipe at the top joint for both normal operating and mooring failure design load cases, under minimum strength and material conditions, is near the compressive yield threshold. If these conditions were to occur, with the first application of maximum bending the pipe will experience a small amount of compressive plastic strain. Additional bending cycles of the same magnitude will have a completely elastic material response. The consequence of yielding in compression is a small loss of tensile yield strength (i.e. yield surface translation). However, for the amount in question, it will not be significant as a) there is margin between the stresses of the high pressure design load cases and autofrettage, and b) the associated plastic strain on fatigue life is small and the occurrence of alternating 100-year hurricane storms and high pressure events should be few.

Stresses in the steel extension between the traplock and the end coupler flange are tabulated in Table 8-11 for each design load case. Allowable end coupler stress per API RP 2RD criteria are provided in Table 8-10. Stresses are within conventional allowables and maximum utilization is at 83 %. The end coupler was originally sized for a higher loading based on a preliminary joint design and global analysis solution. Its design was not optimized.

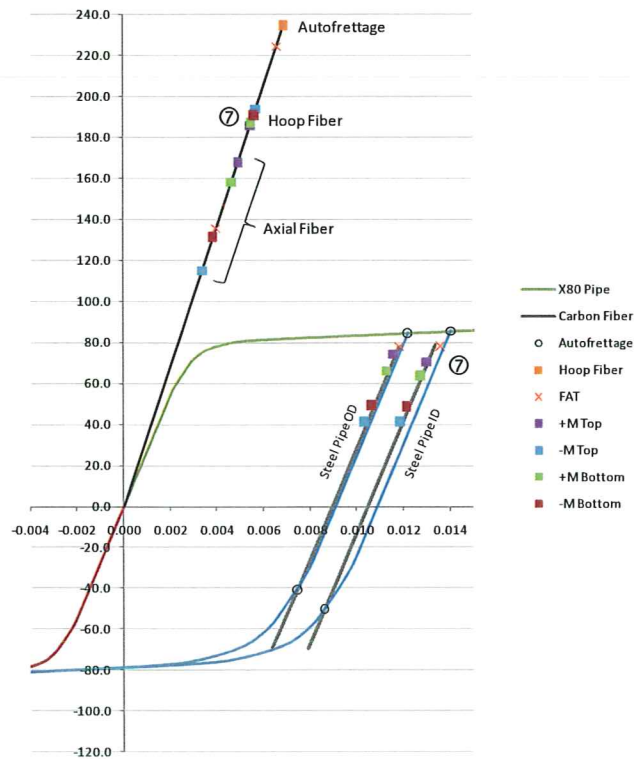


Figure 8-12: Field Pressure Test – Tube Body

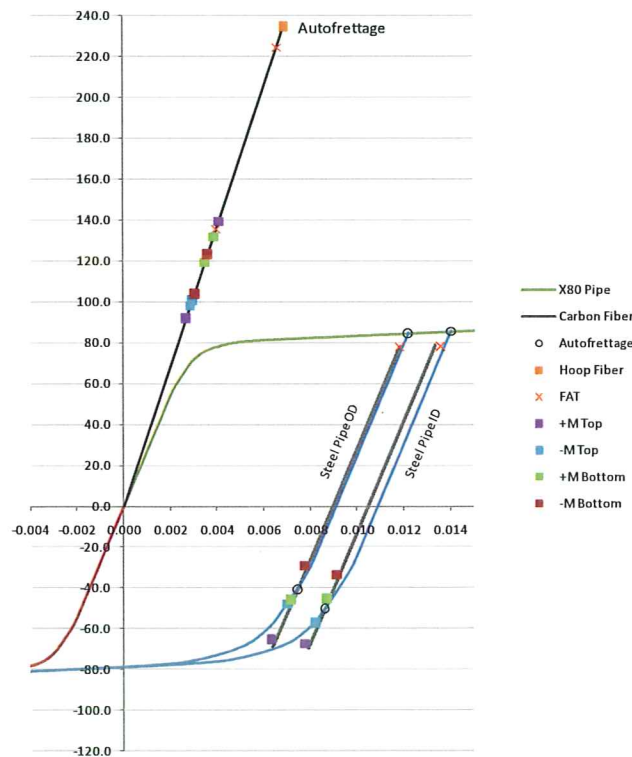


Figure 8-13: Normal Operating – Tube Body

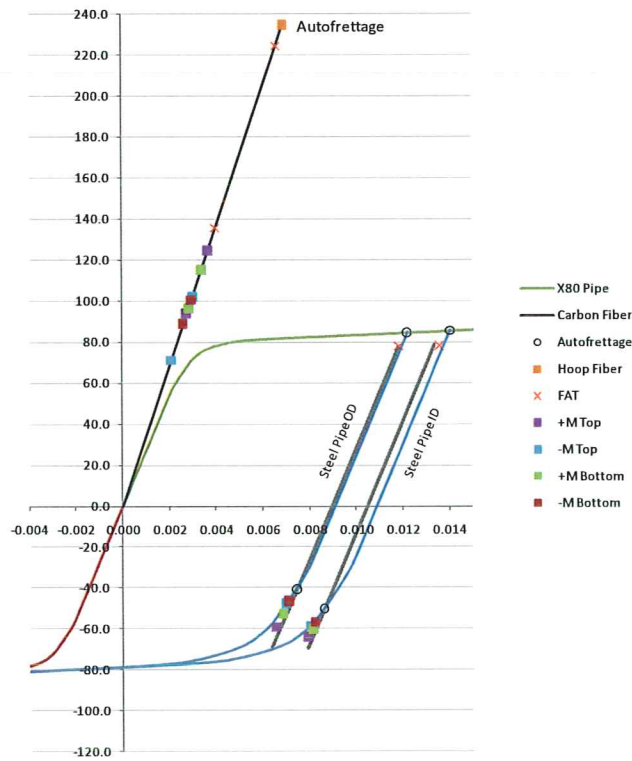


Figure 8-14: Hydrostatic Collapse – Tube Body

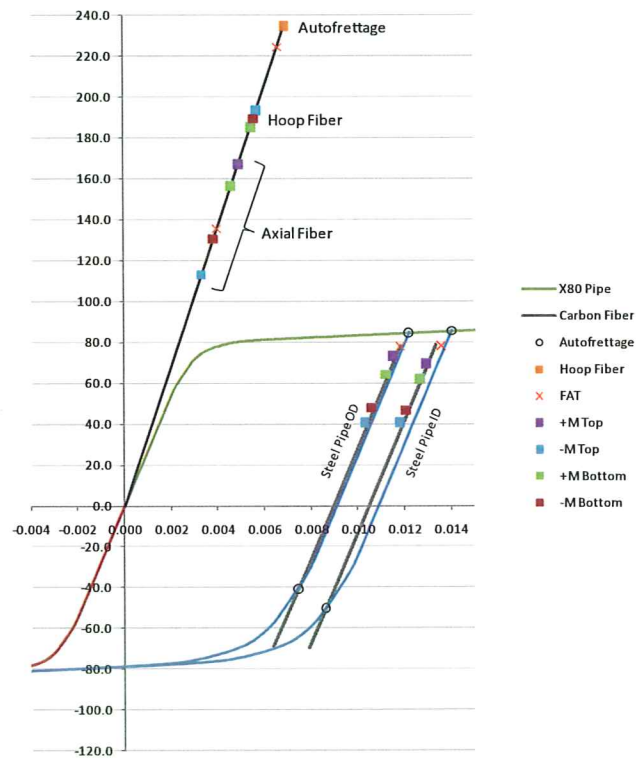


Figure 8-15: Gas Kick – Tube Body

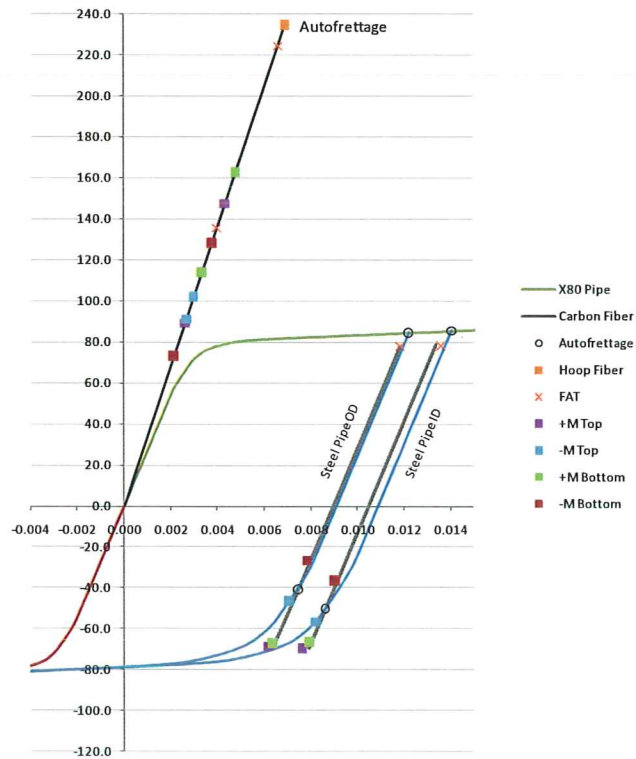


Figure 8-16: Mooring Failure – Tube Body

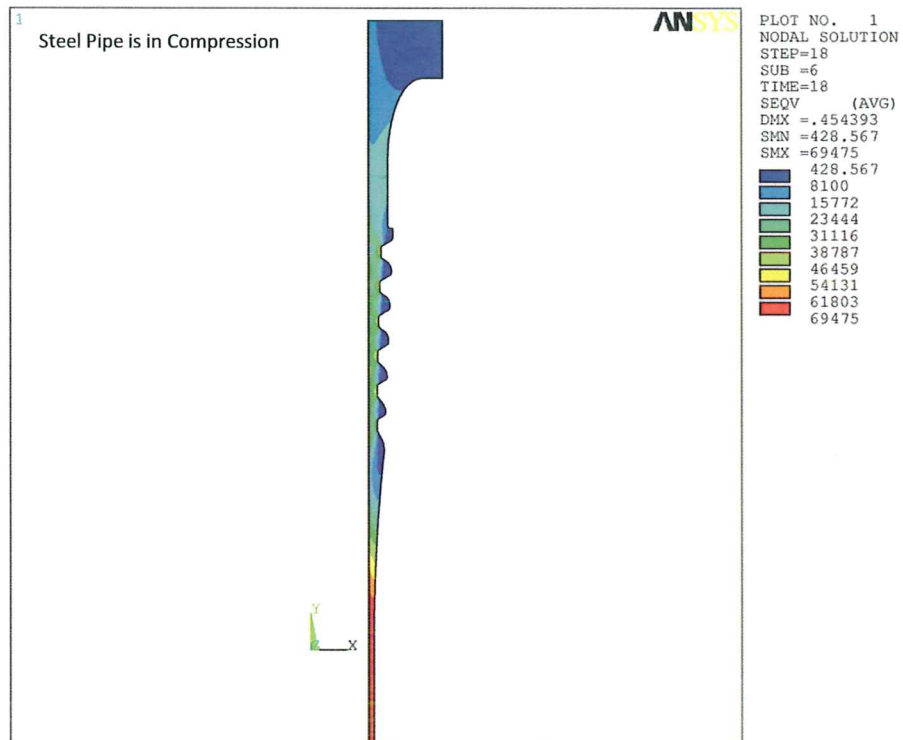


Figure 8-17: +M Top Mooring Failure – Steel Stress



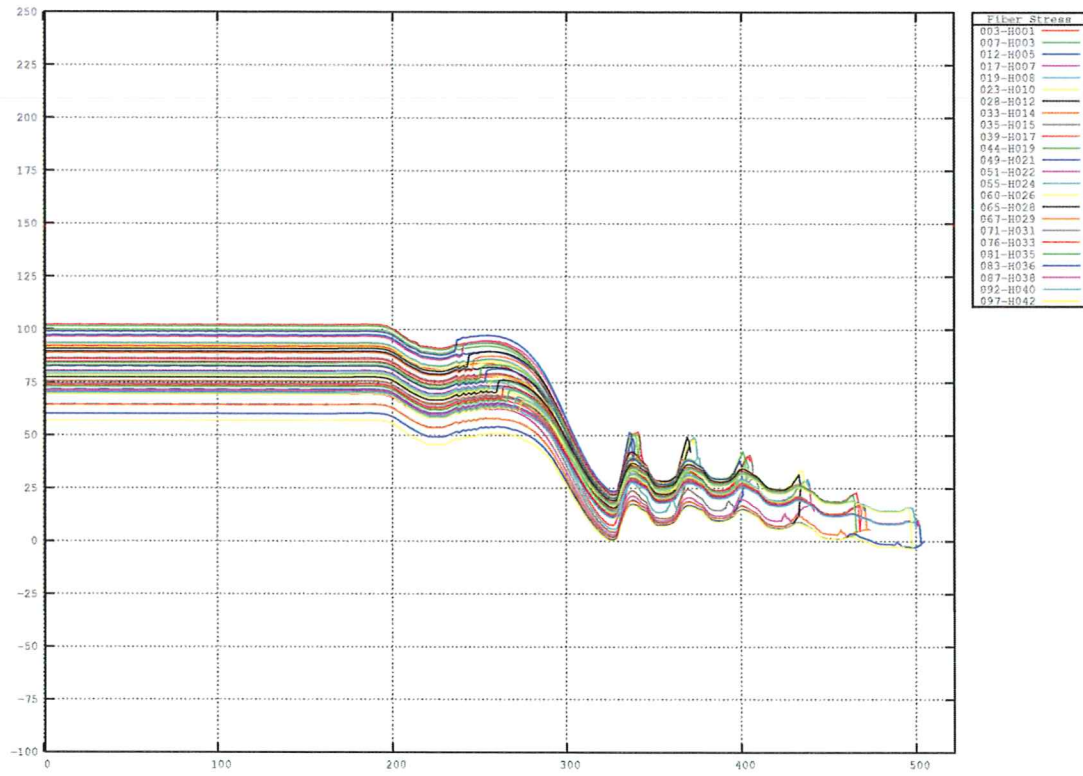


Figure 8-18: -M Top Hydrostatic Collapse - Hoop Fiber Stress

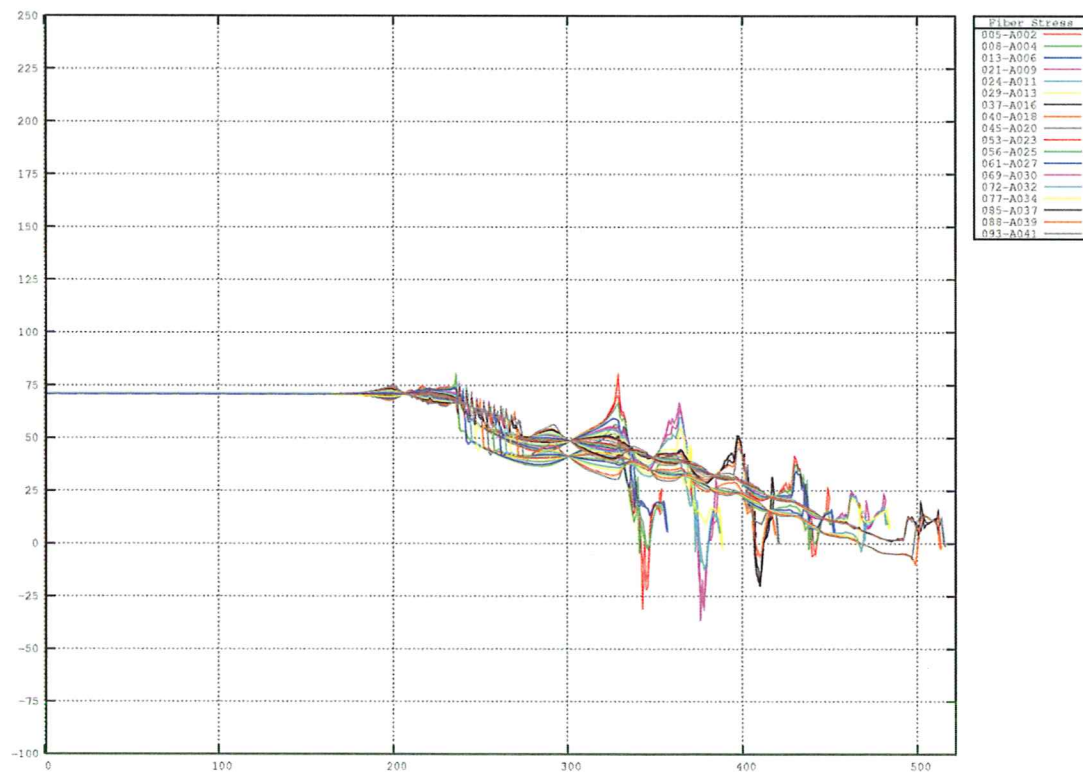


Figure 8-19: -M Top Hydrostatic Collapse - Axial Fiber Stress

**Table 8-6: Composite Fiber Stress Summary**

Load Case	Joint Position <sup>1</sup>	M <sup>2</sup>	SI			USC			A/H Ratio	Util. %	Stress Ratio <sup>3</sup>
			Fiber Stress, MPa			Fiber Stress, ksi					
			Allow.	Hoop	Axial	Allow.	Hoop	Axial			
Autofrettage	NA	1 620	1 617	959	234.9	234.6	139.0	0.59	100	1.92	
Factory Acceptance Test			1 548	935		224.4	135.6	0.60	96	2.00	
Field Pressure Test	T	+	1 280	1 158	200.0	185.6	167.9	0.90	93	2.42	
		-	1 335	792		193.7	114.9	0.59	97	2.32	
	B	+	1 290	1 089		187.0	158.0	0.84	94	2.41	
		-	1 318	907		191.1	131.5	0.69	96	2.35	
Normal Service	T	+	672	818	200.0	97.5	118.6	1.22	59	3.79	
		-	673	812		97.6	117.7	1.21	59	3.82	
	B	+	836	814		121.3	118.0	0.97	61	3.71	
		-	836	813		121.3	117.9	0.97	61	3.71	
Normal Operating	T	+	634	961	200.0	92.0	139.4	1.52	70	3.23	
		-	695	676		100.8	98.1	0.97	50	4.47	
	B	+	822	908		119.2	131.7	1.11	66	3.42	
		-	851	718		123.4	104.1	0.84	62	3.65	
Hydrostatic Collapse	T	+	647	859	200.0	93.8	124.6	1.33	62	3.61	
		-	705	490		102.2	71.1	0.70	51	4.40	
	B	+	665	795		96.4	115.3	1.20	58	3.90	
		-	693	611		100.5	88.7	0.88	50	4.48	
Gas Kick	T	+	1 277	1 152	200.0	185.2	167.1	0.90	93	2.43	
		-	1 335	778		193.6	112.9	0.58	97	2.32	
	B	+	1 278	1 079		185.4	156.5	0.84	93	2.43	
		-	1 306	900		189.4	130.6	0.69	95	2.38	
Mooring Failure	T	+	615	1 016	200.0	89.2	147.4	1.65	74	3.05	
		-	703	628		101.9	91.1	0.89	51	4.42	
	B	+	785	1 123		113.9	162.9	1.43	81	2.76	
		-	884	505		128.2	73.2	0.57	64	3.51	

<sup>1</sup> T-top (keel joint), B-bottom (lower stress joint)

<sup>2</sup> Side relative to the neutral axis (+) tension, (-) compression

<sup>3</sup> Mean fiber strength 3 103 MPa (450 ksi)

**Table 8-7: Allowable Steel Pipe Stress**

Load Case	Load Category	$C_f$	SI			USC		
			Allow. Pipe Stress, MPa			Allow. Pipe Stress, ksi		
			$M^2$	$M+B^3$	$SEqv^4$	$M^2$	$M+B^3$	$SEqv^4$
Factory Acceptance Test	Test	1.35	500	749	1 110	72.5	108.7	161.0
Field Pressure Test	Test	1.35	500	749		72.5	108.7	
Normal Service	Operating	1.00	370	555		53.7	80.5	
Normal Operating	Operating	1.00	370	555		53.7	80.5	
Hydrostatic Collapse	Extreme	1.20	444	666		64.4	96.6	
Gas Kick	Extreme	1.20	444	666		64.4	96.6	
Mooring Failure	Survival	1.50	555	833		80.5	120.8	

<sup>1</sup>  $\sigma_a = C_a \sigma_y$ ;  $C_a = 2/3$ ,  $\sigma_y = 555$  MPa (80.5 ksi)

<sup>2</sup> Membrane ( $C_f \sigma_a$ )

<sup>3</sup> Membrane + Bending ( $1.5 C_f \sigma_a$ )

<sup>4</sup> Von Mises Stress ( $3.0 \sigma_a$ )

**Table 8-8: Steel Pipe Stress Summary**

Load Case	Joint Position <sup>1</sup>	M <sup>2</sup>	SI			USC			Util. %
			Pipe Stress, MPa			Pipe Stress, ksi			
			M <sup>3</sup>	M+B <sup>4</sup>	SEqv <sup>5</sup>	M <sup>3</sup>	M+B <sup>4</sup>	SEqv <sup>5</sup>	
Autofrettage	NA		586	589	589	85.0	85.5	85.5	NA
Factory Acceptance Test			540	540	540	78.3	78.4	78.3	108
Field Pressure Test	T	+	499	513	512	72.3	74.5	74.2	100
		-	284	285	286	41.2	41.3	41.5	57
	B	+	447	456	455	64.8	66.2	66.0	89
		-	338	342	341	49.0	49.6	49.5	68
Normal Service	T	+	-402	-425	-423	-58.3	-61.6	-61.3	109
		-	-403	-428	-426	-58.5	-62.0	-61.8	109
	B	+	-255	-263	-262	-37.0	-38.1	-38.1	69
		-	-255	-262	-262	-36.9	-38.1	-38.0	69
Normal Operating	T	+	-456	-464	-463	-66.1	-67.4	-67.2	123
		-	-361	-396	-394	-52.4	-57.4	-57.1	98
	B	+	-311	-314	-314	-45.1	-45.5	-45.5	84
		-	-231	-231	-230	-30.9	-33.5	-33.4	58
Hydrostatic Collapse	T	+	-424	-442	-439	-61.5	-64.1	-63.7	95
		-	-367	-407	-404	-53.2	-59.0	-58.6	83
	B	+	-387	-414	-413	-56.1	-60.1	-59.9	87
		-	-353	-392	-390	-51.3	-56.8	-56.6	80
Gas Kick	T	+	493	508	506	71.5	73.7	73.4	111
		-	279	279	281	40.4	40.4	40.7	63
	B	+	434	444	443	62.9	64.4	64.2	98
		-	326	331	330	47.2	48.0	47.9	73
Mooring Failure	T	+	-475	-480	-479	-68.9	-69.6	-69.4	86
		-	-355	-392	-390	-51.4	-56.9	-56.6	64
	B	+	-459	-462	-461	-66.6	-67.0	-66.9	83
		-	-215	-251	-250	-31.2	-36.3	-36.2	39

<sup>1</sup> T-top (keel joint), B-bottom (lower stress joint)

<sup>2</sup> Side relative to the neutral axis (+) tension, (-) compression

<sup>3</sup> Membrane

<sup>4</sup> Membrane + Bending

<sup>5</sup> Von Mises Stress

**Table 8-9: Hoop and Axial Components of Pipe Stress**

Load Case	Joint Position <sup>1</sup>	M <sup>2</sup>	SI				USC			
			Pipe Stress, MPa				Pipe Stress, ksi			
			Inside Surface		Outside Surface		Inside Surface		Outside Surface	
			Hoop	Axial	Hoop	Axial	Hoop	Axial	Hoop	Axial
Post Cure Cooldown	NA		0	65	0	65	0.0	9.5	0	9.5
Autofrettage			492	410	516	469	71.4	59.5	74.9	68.0
Post AF Condition			-397	-149	-338	-103	-57.6	-21.6	-49.1	-14.9
Factory Acceptance Test			449	370	469	435	65.2	53.6	68.0	63.1
Post FAT Condition			-396	-154	-338	-100	-57.4	-22.3	-49.0	-14.5
Field Pressure Test	T	+	252	449	261	510	36.6	65.2	37.9	74.0
		-	214	135	219	185	31.1	19.6	31.8	26.8
	B	+	229	358	235	410	33.3	52.0	34.0	59.5
		-	208	199	215	249	30.2	28.8	31.1	36.2
Normal Service	T	+	-431	-9	-368	52	-62.4	-1.3	-53.3	7.5
		-	-430	-1	-369	49	-62.3	-0.1	-53.5	7.2
	B	+	-294	-11	-246	42	-42.6	-1.5	-35.7	6.0
		-	-293	-10	-247	41	-42.5	-1.4	-35.8	6.0
Normal Operating	T	+	-399	112	-343	173	-57.8	16.3	-49.7	25.2
		-	-446	-124	-384	-74	-64.7	-18.0	-55.7	-10.8
	B	+	-283	73	-236	125	-41.0	10.6	-34.2	18.2
		-	-305	-94	-257	-42	-44.2	-13.6	-37.3	-6.2
Hydrostatic Collapse	T	+	-429	23	-370	84	-62.3	3.4	-53.7	12.2
		-	-468	-286	-416	-243	-67.9	-41.5	-60.3	-35.3
	B	+	-464	-70	-402	18	-67.2	-10.2	-58.3	-2.7
		-	-483	-229	-425	-179	-70.1	-33.2	-61.6	-26.0
Gas Kick	T	+	254	443	262	504	36.8	64.2	38.1	73.1
		-	211	122	220	171	30.6	17.7	31.9	24.9
	B	+	216	346	222	398	31.3	50.2	32.2	57.7
		-	195	190	202	241	28.3	27.5	29.3	34.9
Mooring Failure	T	+	-384	155	-330	215	-55.7	22.4	-47.9	31.2
		-	-452	-168	-390	-118	-65.6	-24.4	-56.5	-17.1
	B	+	-259	264	-205	308	-37.5	38.2	-29.8	44.6
		-	-330	-280	-280	-229	-47.8	-40.7	-40.7	-33.3

<sup>1</sup> T-top (keel joint), B-bottom (lower stress joint)

<sup>2</sup> Side relative to the neutral axis (+) tension, (-) compression



**Table 8-10: Allowable Steel End Coupler Stress**

Load Case	Load Category	$C_f$	SI			USC		
			Allow. Coupler Stress, MPa			Allow. Coupler Stress, ksi		
			$M^2$	$M+B^3$	$SEqv^4$	$M^2$	$M+B^3$	$SEqv^4$
Factory Acceptance Test	Test	1.35	465	698	1 034	67.5	101.3	150.0
Field Pressure Test	Test	1.35	465	698		67.5	101.3	
Normal Operating	Operating	1.00	345	517		50.0	75.0	
Hydrostatic Collapse	Extreme	1.20	414	621		60.0	90.0	
Gas Kick	Extreme	1.20	414	621		60.0	90.0	
Mooring Failure	Survival	1.50	517	776		75.0	112.5	

<sup>1</sup>  $\sigma_a = C_a \sigma_y$ ;  $C_a = 2/3$ ,  $\sigma_y = 517$  MPa (75.0 ksi)

<sup>2</sup> Membrane ( $C_f \sigma_a$ )

<sup>3</sup> Membrane + Bending ( $1.5 C_f \sigma_a$ )

<sup>4</sup> Von Mises Stress ( $3.0 \sigma_a$ )

**Table 8-11: Steel End Coupler Stress Summary**

Load Case	Joint Position <sup>1</sup>	M <sup>2</sup>	SI			USC			Util. %
			Coupler Stress, MPa			Coupler Stress, ksi			
			M <sup>3</sup>	M+B <sup>4</sup>	SEqv <sup>5</sup>	M <sup>3</sup>	M+B <sup>4</sup>	SEqv <sup>5</sup>	
Autofrettage	NA		411	491	482	59.6	71.3	69.9	NA
Factory Acceptance Test	NA		385	458	449	55.8	66.4	65.1	83
Field Pressure Test	T	+	320	371	360	46.4	53.7	52.3	69
		-	310	360	349	44.9	52.2	50.6	67
	B	+	320	372	361	46.3	53.9	52.4	69
		-	311	362	352	45.1	52.6	51.0	67
Normal Service	T	+	73	87	97	10.6	12.6	14.0	21
		-	73	87	97	10.6	12.6	14.0	21
	B	+	101	106	98	14.6	15.4	14.2	29
		-	101	106	98	14.6	15.4	14.2	29
Normal Operating	T	+	115	129	137	16.7	18.7	19.8	33
		-	31	48	62	4.5	7.0	8.9	9
	B	+	121	122	117	17.5	17.6	16.9	35
		-	87	97	87	12.6	14.1	12.6	25
Hydrostatic Collapse	T	+	86	103	113	12.5	15.0	16.4	21
		-	25	43	56	3.6	6.3	8.2	7
	B	+	78	97	107	11.3	14.1	15.5	19
		-	23	49	63	3.3	7.0	9.1	8
Gas Kick	T	+	319	369	359	46.3	53.6	52.1	77
		-	310	360	349	44.9	52.2	50.6	75
	B	+	313	364	354	45.5	52.8	51.3	76
		-	305	355	344	44.2	51.5	49.9	74
Mooring Failure	T	+	130	144	152	18.9	20.9	22.0	25
		-	16	38	53	2.4	5.5	7.6	5
	B	+	174	182	180	25.2	26.5	26.1	34
		-	87	103	92	12.7	15.0	13.4	17

<sup>1</sup> T-top (keel joint), B-bottom (lower stress joint)

<sup>2</sup> Side relative to the neutral axis (+) tension, (-) compression

<sup>3</sup> Membrane

<sup>4</sup> Membrane + Bending

<sup>5</sup> Von Mises Stress

## Cyclic Fatigue

Fatigue of the steel pipe was evaluated using a strain-life model developed by Manson and Hirschberg<sup>9</sup> known as the method of universal slopes (MUS), relating life  $N$  to a given strain range  $\Delta\epsilon$  for a fully reversing load ( $R = -1$ ). The equation is appropriate for both high cycle ( $N > 10^3$ ) and low cycle ( $1 \leq N \leq 10^3$ ) fatigue damage.

$$\Delta\epsilon = 3.5 \frac{\sigma_u}{E} N^{-0.12} + D^{0.6} N^{-0.6}$$

$$D = \ln\left(\frac{100}{100 - RA}\right)$$

where,

$N$	Number of cycles to failure
$\Delta\epsilon$	Strain range of a cycle
$\sigma_u$	Ultimate tensile strength
$E$	Tensile modulus
$D$	Ductility coefficient
$RA$	Reduction of area, %

Using material values listed in Table 7-1 and a minimum strength of 625 MPa (90.6 ksi), Figure 8-20 is generated.

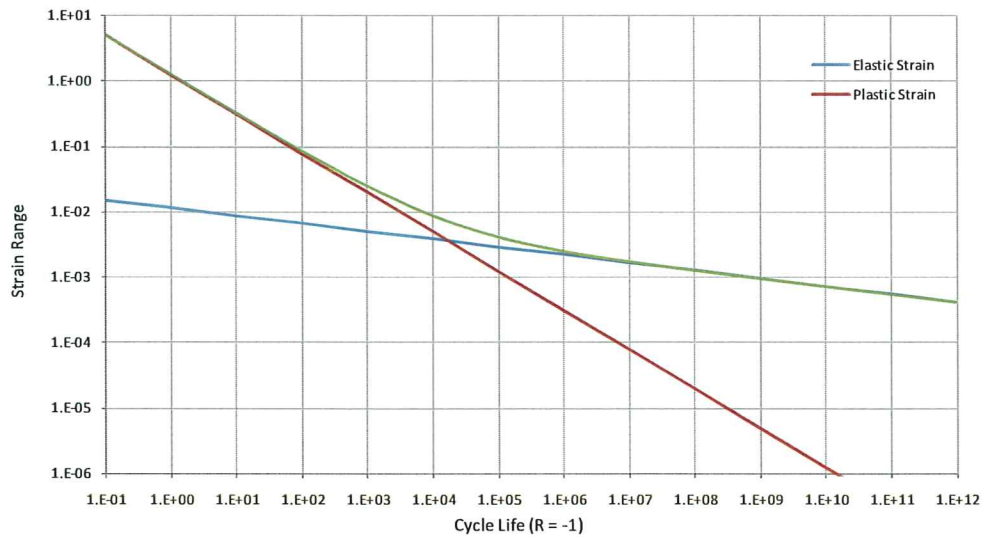


Figure 8-20: Strain-life Fatigue Curve

Fatigue life was assessed considering the effects of autofrettage, factory acceptance test, and high pressure design load cases using the cycle counts listed in Table 8-5; and an infinite number of normal operating cycles of maximum bending (fully reversed). Load conditions are as previously defined (100-year hurricane, 1.9 % offset). Results are listed in Table 8-12. Strain ranges are based on FE results for the tube body. The Palmgren-Miner linear damage model was used to solve for the number of normal operating cycles resulting in unity using a design fatigue factor (DFF) of 10 on life. The limiting number of bending cycles is  $1.71\text{E}+09$  (+M Top), indicating the load is below the endurance limit of the material. This is consistent with a fatigue strength of roughly 50 % of ultimate and considering the axial stresses listed in Table 8-9 for the normal operating design load case.

<sup>9</sup> S.S. Manson, *Fatigue: A Complex Subject – Some Simple Approximations*; Proceedings, Society of Experimental Stress Analysis, Vol. 12, No. 2, 1965

This is a conservative assessment considering extreme loads have been used instead of the more mild sea states making up the majority of life, and it assumes conditions never change (wave heading, joint location in the string).

**Table 8-12: Pipe Fatigue Summary**

Load Case	+M Top					
	Inside Surface			Outside Surface		
	$\Delta\epsilon$	Life, N	Cycles	$\Delta\epsilon$	Life, N	Cycles
Autofrettage	0.014032	3387	0.5	0.012211	4644	0.5
Post AF Condition	0.005404	41748	0.5	0.004763	63817	0.5
Factory Acceptance Test	0.004984	54588	1	0.004406	84370	1
Field Pressure Test	0.004355	88075	80	0.004136	106999	80
Gas Kick	0.004305	92021	2	0.004089	111925	2
Normal Operating	0.000423	1.07E+12	1.06E+11	0.000695	1.73E+10	1.71E+09
Miner Sum (DFF =10)			1			1

Load Case	-M Top					
	Inside Surface			Outside Surface		
	$\Delta\epsilon$	Life, N	Cycles	$\Delta\epsilon$	Life, N	Cycles
Autofrettage	0.014032	3387	0.5	0.012211	4644	0.5
Post AF Condition	0.005404	41748	0.5	0.004763	63817	0.5
Factory Acceptance Test	0.004984	54588	1	0.004406	84370	1
Field Pressure Test	0.003201	316157	80	0.002899	511954	80
Gas Kick	0.003167	332349	2	0.002858	550314	2
Normal Operating	0.000423	1.07E+12	1.07E+11	0.000695	1.73E+10	1.72E+09
Miner Sum (DFF =10)			1			1

Load Case	+M Bottom					
	Inside Surface			Outside Surface		
	$\Delta\epsilon$	Life, N	Cycles	$\Delta\epsilon$	Life, N	Cycles
Autofrettage	0.014032	3387	0.5	0.012211	4644	0.5
Post AF Condition	0.005404	41748	0.5	0.004763	63817	0.5
Factory Acceptance Test	0.004984	54588	1	0.004406	84370	1
Field Pressure Test	0.004086	112137	80	0.003844	142953	80
Gas Kick	0.004010	120655	2	0.003777	153408	2
Normal Operating	0.000425	1.03E+12	1.02E+11	0.000606	5.45E+10	5.42E+09
Miner Sum (DFF=10)			1			1

Load Case	-M Bottom					
	Inside Surface			Outside Surface		
	$\Delta\epsilon$	Life, N	Cycles	$\Delta\epsilon$	Life, N	Cycles
Autofrettage	.014032	3387	0.5	.012211	4644	0.5
Post AF Condition	.005404	41748	0.5	.004763	63817	0.5
Factory Acceptance Test	.004984	54588	1	.004406	84370	1
Field Pressure Test	.003513	208195	80	.003229	304066	80
Gas Kick	.003442	227605	2	.003169	331857	2
Normal Operating	.000425	1.03E+12	1.02E+11	.000606	5.45E+10	5.43E+09
Miner Sum (DFF =10)			1			1



## 9. Design Verification

Design verification was performed by prototyping full-diameter test articles, for the purpose of demonstrating manufacturability of the design (materials, process) and to assess performance with respect to burst strength, fatigue, and tolerance to impact damage.

### Prototype Configuration

Three full-diameter half length test prototypes were built. The length of prototypes provided a tube body distance greater than the required six diameters. In all respects prototypes were structurally identical to the design, except the coupler flange was replaced with a 752 mm (29.6 inch) constant outside diameter to interface with bending equipment, and the inside bore was modified to accept a high pressure end plug assembly. The outer HNBR layer and sacrificial glass top layer were omitted. A section view of the prototype end coupler is illustrated in Figure 9-1.

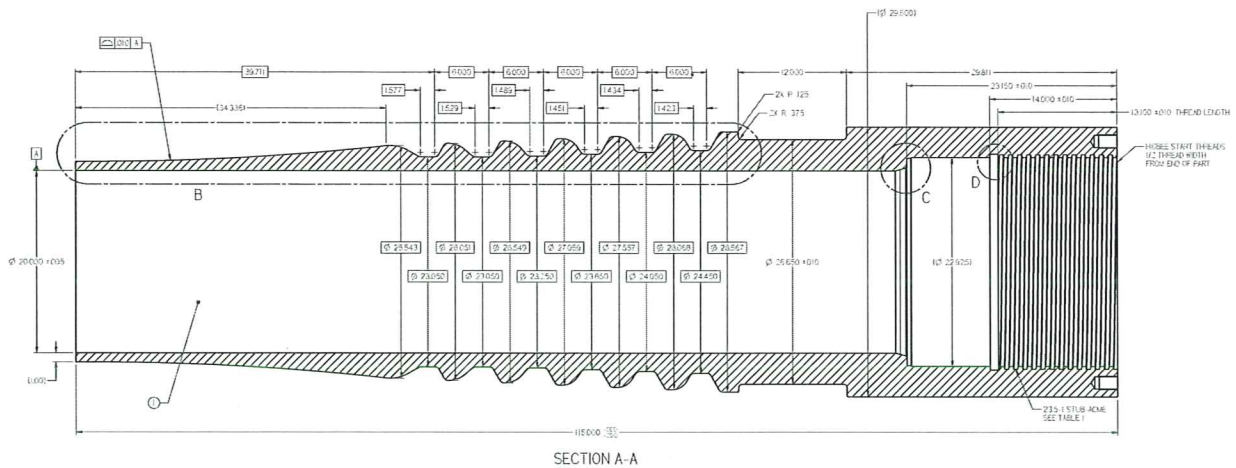


Figure 9-1: Prototype End Coupler

The X80 pipe was material manufactured by Sumitomo Corporation but rejected by the intended customer due to weld repair. No specific information was available as to the nature of the repair, however the pipe was said to comply with the requirements of API 5L for grade PSL2. Pipe yield and ultimate strength were 600 MPa (87 ksi) and 738 MPa (107 ksi) respectively, based on the manufacturers inspection certificate for the lot. Independent testing of the pipe purchased confirmed these values. Pipe dimensions were at nominal values ( $\varnothing 559 \times 25.4$  mm,  $\varnothing 22 \times 1$  inch). Measured out-of-roundness was 1.9 mm (0.075 inch).

End couplers were spindle forged by Scot Forge using available material meeting F22 mechanical requirements and closely matching chemistry, however not strictly within specification. Yield and ultimate strength of forgings were 690 MPa (100 ksi) and 800 MPa (116 ksi) respectively. Forgings were ultrasonic inspected (UT) per ASME SA-388, 100 % coverage, all indications marked. No significant defects were found.

Welding was performed by RTI International. Although the length of pipe purchased allowed a continuous tube body section, to maintain consistency with the design, the pipe was cut and remade to include a mid-length girth weld. Longitudinal weld seams were offset. Girth welds joining end coupler-to-pipe and pipe-to-pipe welds were single-sided; using a GTAW root, SMAW hot, and SAW fill and cap process. Weld consumables meet post weld heat treatment (PWHT) strength requirements and allowable nickel content for sour service (NACE MR0175). Both procedures are based on qualified welds; however the specific welds made were not.



Girth welds were conditioned inside and out, flush with the base material. The longitudinal pipe seam was also conditioned on the outside diameter to reduce reinforcement height and to blend out the toe. Typical wall thickness after grinding was 24,4 mm (0.96 inch). Peaking of the pipe seam resulted in several welds failing to meet the minimum required wall thickness at girth welds. These areas were reworked to provide a minimum wall thickness of 23,9 mm (0.94 inch) based on the minimum allowable pipe wall thickness per API 5L.

The steel assembly was cleaned per SSPC-SP6 (commercial blast) and coated with a black polyurethane paint to protect from surface corrosion prior to winding. Winding was performed according to design. Dimensional and weight measurements for each of the three prototypes are listed in Table 9-1. Actual weights were within a few percent of the calculated value. Figure 9-2 is a photograph of a prototype.

**Table 9-1: Prototype Measurements**

	SI				USC			
	Design	SN1	SN2	SN3	Design	SN1	SN2	SN3
Length	10 973 mm	10 975 mm	10 980 mm	10 973 mm	432.0 inch	432.1 inch	432.3 inch	432.0 inch
Tube Body Diameter	663 mm	660 mm	660 mm	666 mm	26.1 inch	26.0 inch	26.0 inch	26.2 inch
Wall Thickness	77,2 mm	76,0 mm	76,7 mm	79,0 mm	3.04 inch	2.99 inch	3.02 inch	3.11 inch
Steel Weight	7 545 kg	7 525 kg	7 521 kg	7 523 kg	16,634 lb	16,590 lb	16,582 lb	16,586 lb
Composite Weight	1 451 kg	1 442 kg	1 287 kg	1 387 kg	3,199 lb	3,180 lb	2,838 lb	3,057 lb
Total Weight	8 996 kg	8 968 kg	8 809 kg	8 910 kg	19,833 lb	19,770 lb	19,420 lb	19,643 lb
Averaged Weight	819,8 kg/m	817,1 kg/m	802,3 kg/m	812,0 kg/m	550.9 lb/ft	549.0 lb/ft	539.1 lb/ft	545.6 lb/ft



**Figure 9-2: Full-diameter Prototype**

## Test Program

Three tests were performed: a pressure burst test, a combined tension-bending cycle test, and a dropped object impact test. All tests were performed by Stress Engineering Services at their Waller Texas facility.

### Pressure Burst Test

After completing autofrettage and factory acceptance test pressure cycles, prototype SN1 was preconditioned with twenty pressure cycles to 110 % of MAOP (113,8 MPa, 16,500 psi) prior to bursting. On the final ramp to burst, a maximum pressure of 258,6 MPa (37,500 psi) was reached before aborting the test due to failure of one of the end plug seals. SN1 remains fully intact.

The test was analyzed using the same FE model as previously described for local analysis, except actual steel yield strength and wall thickness were substituted for design minimums. Results for the tube body section are plotted in Figure 9-3. Stresses are in USC units of ksi. The range of stress and strain during pressure cycling is marked by green triangles. The range marked for carbon fiber is of the higher stressed hoop fibers.

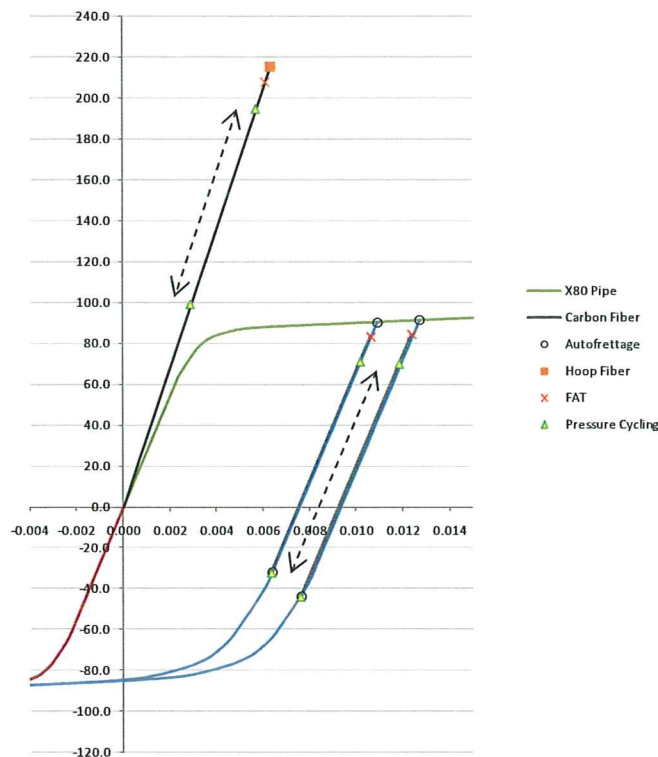
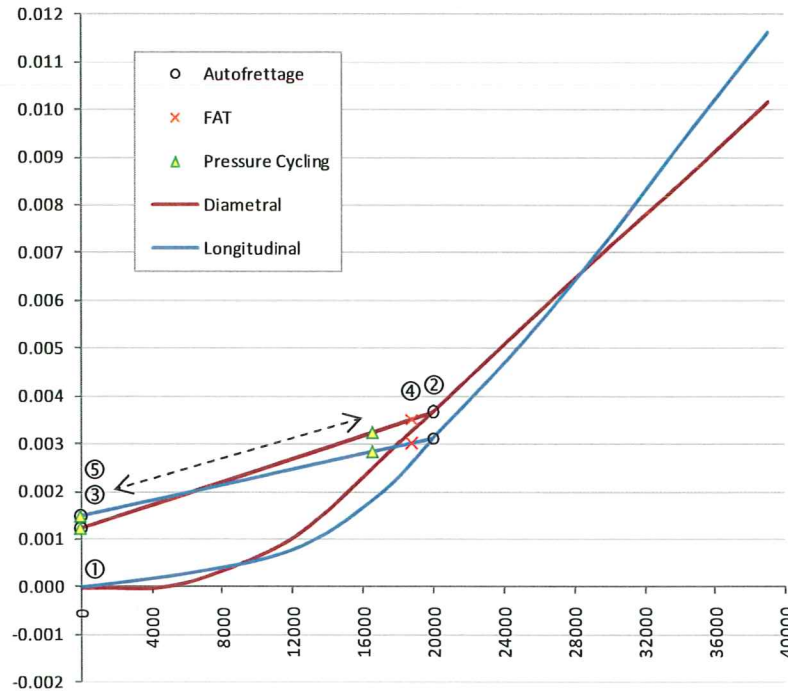


Figure 9-3: Pressure Cycling – Tube Body

The corresponding diametral and longitudinal strains at the outside surface are plotted in Figure 9-4. Pressure is in USC units of psi. Autofrettage begins at zero strain and increases with pressure up to 82,7 MPa (12,000 psi), at which point the steel begins to expand plastically. Diametral strain to 34,5 MPa (5,000 psi) is zero, until dilation of the steel pipe closes the post cure radial gap and bears against composite. After autofrettage pressure has been reached, pressure is released, and the material unloads elastically. The following factory acceptance test cycle and twenty preconditioning cycles have a purely elastic response. For pressures above autofrettage the slope changes as steel load share returns to fully plastic behavior.



**Figure 9-4: Pressure Burst Test – Surface Strain v. Pressure**

Prior to testing, the tube body was instrumented to measure strain. Measurements during each step of testing were consistent with the analytical model. Factory acceptance test pressure was held for eight hours. During this time strains were constant. For each of the twenty preconditioning cycles, strain measurements traced overtop preceding cycles.

Results of the pressure burst test verified the autofrettage process, elastic behavior to factory acceptance test pressure, fully recoverable cycles to MAOP, and sufficient margin of safety with respect to burst strength.

#### **Combined Tension-Bending Cycle Test**

After completing autofrettage and factory acceptance test pressure cycles, prototype SN2 was subjected to 100 000 bending cycles of the normal operating design load case for a top joint (critical location based on fatigue analysis). A bending moment cycle of -759 to +997 kN-m (-560 to +735 kip-ft) was applied to simulate the maximum range of the global analysis solution (static +/- dynamic). An internal pressure of 53,7 MPa (7,790 psi) was held constant to apply the equivalent of 10,82 MN (2,433 kip) axial tension. Figure 9-5 is a photograph of the bending fixture. All bending cycles were completed successfully.

SN2 was then pressurized to failure. Burst pressure was 269,9 MPa (39,100 psi, 2.60 burst ratio) with a hoop failure mode. Failure initiated along a longitudinal pipe seam, separating the weld from the base material. Figure 9-6 is a photograph of the area. The opposite pipe section fish-mouthed. All three girth welds and the MCI at both ends were intact. Fiber stress at burst demonstrated a 71 % strength translation (60 % assumed in design).

Results of the combined tension-bending cycle test demonstrated sufficient margin of safety with respect to fatigue performance by withstanding the equivalent of many 100-year hurricane storms with no apparent degradation in strength.





**Figure 9-5: Combined Tension-Bending Cycle Test**



**Figure 9-6: Burst Carcass**



### Dropped Object Impact Test

After completing autofrettage and factory acceptance test pressure cycles, prototype SN3 was impacted unpressurized with 68kJ (50 kipf-ft) of energy. Impacts were placed in three critical locations:

- At the pipe-to-pipe girth weld in the middle of the tube body
- Over the innermost MCI trap groove at the location of highest fiber stress (end A)
- At the end coupler-to-pipe girth weld (end B)

Each impact was made by dropping a striker weighted to 4 536 kg (10,000 lb) from a height of 1,5 m (5 ft). Shape of the striker was a 102 mm (4 inch) thick steel plate beveled 45 deg to a sharp edge and oriented to strike across the diameter. Figure 9-7 is a photograph of the test fixture, with an inset showing typical damage after impact.



**Figure 9-7: Dropped Object Impact Test**

After all three impacts were made, SN3 was pressure tested to MAOP and held for 30 minutes, followed by the 100 000 combined tension-bending cycle test performed on SN2, and then a second pressure test to MAOP. Each step was completed successfully and any progression of impact damage was not visually apparent.

SN3 was then pressurized to failure. Burst pressure was 174,4 MPa (25,300 psi). Failure initiated with the loss of composite integrity around the MCI impact, leading to axial failure of the steel end coupler near the girth weld.

Results of this test are considered a success, having demonstrated a working prototype after the equivalent of many 100-year hurricane storms in a severely damage condition. Burst strength after cycling showed integrity to a pressure of 169 % of MAOP. The pressure end force at burst was 35,4 MN (7,948 kipf).

## 10. Conclusion

A lightweight dry tree drilling riser system has been designed using composite materials as a principal structural member for the purpose of reinforcing conventional marine riser technology for ultra-deepwater and high pressure applications. The presented riser system is suitable for existing tension-leg (TLP) or spar platforms using industry standard equipment.

This work has confirmed preceding investigations suggesting a potential weight savings of 40-50 % in comparison to all steel construction. Full-diameter prototypes have demonstrated manufacturability and sufficient margins of safety with respect to burst strength, bending fatigue, and tolerance to dropped object impact damage.

The next phase of this project is to work with industry and regulatory authorities to define a design qualification framework that will establish a TRL 6-7 in accordance with API 17N. The scope of this phase will be to address differences in composite versus conventional riser design philosophy, to prepare a risk mitigation plan according to DNV RP-A203 *Qualification Procedures for New Technology*, and to execute this plan in preparation for field trial.

## Contact Information

### Program Manager

Donald D. Baldwin

Director, Product Development

### Contract Manager

Chet M. Dawes

Director, North America Sales

### Project Manager

Jon E. Knudsen

Project Engineer

### Design and Development

Chad A. Cederberg

Design Engineer

Lincoln Composites, Inc.

A Member of Hexagon Composites Group

5117 NW 40<sup>th</sup> ST

Lincoln, NE 68524

1 (402) 470-5000